The uncharacterized protein YgfB contributes to β-lactam resistance in *Pseudomonas aeruginosa* by inhibiting the expression of the amidase AmpDh3

Ole Eggers[1], Fabian Renschler[1,2], Lydia Anita Michalek[1], Noelle Wackler[1], Elias Walter[1], Fabian Smollich[1], Kristina Klein[1], Michael Sonnabend[1,3], Valentin Egle[1,5], Angel Angelov[3], Christina Engesser[3], Marina Borisova[4,5], Christoph Mayer[4,5], Monika Schütz[1,2] and Erwin Bohn[1,2,5*]

[1]Institute for Medical Microbiology and Hygiene, Interfaculty Institute of Microbiology and Infection Medicine (IMIT), Eberhard Karls University Tübingen.

[2]German Centre for Infection Research (DZIF), Partner Site Tübingen, Tübingen, Germany.

[3]NGS Competence Center Tübingen (NCCT), Institute for Medical Microbiology and Hygiene, Eberhard Karls University Tübingen.

[4]Department of Biology, Organismic Interactions/Glycobiology, Interfaculty Institute of Microbiology and Infection Medicine (IMIT), Eberhard Karls University Tübingen.

[5]Cluster of Excellence "Controlling Microbes to Fight Infections" University of Tübingen, Tübingen, Germany.

Running title: Impact of YgfB on antibiotic resistance

***Correspondence:**

Dr. rer. nat. Erwin Bohn

erwin.bohn@med.uni-tuebingen.de

Keywords: *Pseudomonas aeruginosa*, YgfB, AmpDh3, AlpA, β-lactam resistance, MDR, ciprofloxacin

Abstract

YgfB was recently identified as an enigmatic factor that contributes to β-lactam resistance of multi drug resistant *Pseudomonas aeruginosa*. We show here that YgfB upregulates the expression of the chromosomally encoded β-lactamase AmpC by antagonizing the function of the regulator of the programmed cell death pathway AlpA. As an anti-terminator, AlpA induces the expression of the *alpBCDE* lysis genes and the amidase AmpDh3. AmpDh3 activity in turn reduces the levels of cell wall-derived 1,6-anhydro-N-acetylmuramyl-peptides (anhMurNAc-peptides), which stimulate the activator function of the transcriptional regulator AmpR, thereby promoting the expression of *ampC* and β-lactam resistance. Furthermore, we demonstrate that ciprofloxacin-mediated DNA damage induces AlpA-dependent production of AmpDh3, thereby reducing the minimal inhibitory concentration of β-lactam antibiotics required to kill *P. aeruginosa*. YgfB is also instrumental in dampening this synergistic action. Altogether, our work highlights the contribution of YgfB to β-lactam and ciprofloxacin/β-lactam resistance and pinpoints a new potential antimicrobial target.

Introduction

The rise in multi drug resistance (MDR) represents a major public health issue due to declining options for the treatment of bacterial infections. This poses a large problem particularly for nosocomial infections with *P. aeruginosa* (*Pa*), which is one of the most important Gram-negative pathogens and a major cause of pneumonia, urinary tract infections, wound infections and blood stream infections. *Pa* employs various intrinsic and acquired antibiotic resistance mechanisms. The high intrinsic resistance is mainly the result of a very low permeability of the outer membrane[1] and the inducible expression of efflux pumps[2]. High-level β-lactam resistance, including resistance to carbapenems and cephalosporins, is mediated by the upregulation of the chromosomally-encoded cephalosporinase AmpC[2]. While low in wild type *Pa* strains, the levels of *ampC* are often strongly increased in clinical isolates. This derepression of *ampC* can be caused by mutations in *ampR*, which encodes the transcriptional regulator AmpR, as well as in the genes *ampD,* encoding a muropeptide amidase[3, 4], or *dacB*,

encoding the penicillin-binding protein 4 (PBP4)[5]. Additionally, *ampC* expression can be induced by β-lactam antibiotics and β-lactamase inhibitors. This can result in resistance to most β-lactam antibiotics[6]. AmpR regulates *ampC* expression by sensing the relative amounts of peptidoglycan (PG) recycling metabolites and synthesis precursors[7]. When bound to UDP-N-acetylmuramic acid pentapeptide (UDP-MurNAc-pentapeptide), the final soluble PG synthesis precursor, AmpR[8] represses the expression of a subset of genes such as *ampC*. On the contrary, 1,6-anhydro-N-acetyl-MurNAc-peptides (anhMurNAc-peptides) originating from the turnover and recycling of the PG cell wall[9] can displace UDP-MurNAc-pentapeptide from AmpR. This allows AmpR to transactivate various promoters such as the *ampC* promoter. Interestingly, those mutations in *ampD* or *dacB* that cause derepression of *ampC* lead to a rise in the intracellular pool levels of anhMurNAc-peptides such as 1,6-MurNAc-L-alanyl-D-glutamyl-meso-diaminopimelic acid-D-alanyl-D-alanine, i.e., anhMurNAc-pentapeptide[7].

The MDR *Pa* strain ID40 is a bloodstream isolate carrying a loss of function mutation in *dacB* which inactivates Penicillin binding protein 4 (PBP4)[10, 11]. In a recent approach we identified various genes that contribute to resistance toward β-lactam antibiotics in ID40. Among them is the so far uncharacterized gene *ygfB*, whose expression significantly increases the levels of AmpC, β-lactamase activity and consequently, resistance to various classes of β-lactam antibiotics such as carbapenems, monobactams, and 3rd and 4th generation cephalosporins[10]. YgfB belongs to the UPF0149 family of proteins and orthologs are found in many γ-proteobacteria (Fig. S1). YgfB consists of seven α-helices and the structure analysis of the *Haemophilus influenzae* ortholog suggests that YgfB forms a homodimer (PDB ID 1IZM[12]). To this point and to our knowledge, nothing else is currently known about the function of YgfB proteins.

In the present study, we unraveled how YgfB contributes to β-lactam resistance. We show that in *P. aeruginosa* YgfB decreases the production levels of the amidase AmpDh3 by antagonizing the activity of the anti-terminator protein AlpA, which controls the expression of AmpDh3. This role of YgfB seems to be conserved across different clinical isolates of *Pa.*

Furthermore, we provide a molecular explanation to why the ciprofloxacin/β-lactam combination therapy is ineffective in many cases of *Pa* infections.

Results

Transcriptomic analysis reveals specific effects of YgfB on gene expression

To investigate the role of YgfB in antibiotic resistance, a transcriptome analysis was performed using next generation sequencing with mRNAs isolated from ID40 and the isogenic *ygfB* null mutant ID40Δ*ygfB*. As depicted in **Table 1**, the mRNA expression of only a few genes was significantly altered following *ygfB* deletion, indicating a very specific effect of YgfB on the transcriptional level.

In particular, deletion of *ygfB* resulted in the downregulation of only one gene, *ampC*, encoding the β-lactamase, and the upregulation of seven other genes including the *ampDh3*-TUEID40_01954 operon, a gene encoding a glyoxalase-like protein and the *alpBCDE* genes. Together with its paralogues AmpD and AmpDh2, AmpDh3 belongs to the family of amidases that are able to remove the peptide stem from peptidoglycan intermediates[13]. All of them were described to contribute to β-lactam resistance[14]. Additionally, AmpDh3 acts as an effector protein that is translocated into competing bacteria by a type VI secretion system (T6SS), thereby contributing to the lysis of prey bacteria via its amidase activity[15]. PA0808 (orthologue of TUEID40_01954 in the strain PAO1) was described as a periplasmic immunity protein which binds and thereby antagonizes the amidase activity of AmpDh3. AlpA was recently described to be an anti-terminator that transcriptionally regulates the *alpBCDE* cluster, encoding a self-lysis pathway, and the *ampDh3* operon. The activation of the self-lysis pathway can occur in a subset of cells in response to DNA damage, is lethal to the individual cells in which it occurs and might be required to enhance pathogenicity during lung infection[16]. Positive regulation of the expression of both the *alpBCDE* and *ampDh3* cluster can be induced by ciprofloxacin-mediated DNA damage[16, 17]

Since it was shown that AlpA specifically upregulates the expression of both the *alpBCDE* cluster and *ampDh3*, we speculated that YgfB could be a negative regulator of AlpA-mediated

transcription[16, 17]. Based on the amidase function of AmpDh3 we hypothesized that *ygfB* deletion could increase the AmpDh3 levels, thereby leading to a reduction in the levels of anhMurNAc-peptides. This would in turn lead to a reduction in the transcriptional activation of *ampC* by AmpR and an increased sensitivity to β-lactam antibiotics.

Validation of transcriptomics results by RT-qPCR and Western blots

The transcriptomics results were validated by RT-qPCR and Western blot analysis. For this purpose, we compared mRNA and protein levels across the strains ID40, ID40Δ*ygfB* and ID40Δ*ygfB* complemented with an genomic copy of *ygfB* under the control of a rhamnose inducible promoter (Δ*ygfB::*rha-*ygfB*) **(Fig. 1a and b)**. We found that *ygfB* deletion significantly reduced the expression of *ampC* and increased the expression of the operon encoding for *ampDh3* and TUEID40_01954 **(Fig. 1a)**. Complementation was achieved by the addition of various concentrations of rhamnose, leading to increased *ygfB* and *ampC* expression and a parallel decrease in the expression of *ampDh3* and TUEID40_01954. The expression of the *ampDh3* paralogues *ampD* and *ampDh2* was not affected by the *ygfB* deletion. While we could see a clear effect of *ygfB* deletion on the mRNA expression of the *alpBCDE* genes in transcriptomic analysis, only a subtle, non-significant impact of YgfB expression on the *alpBCDE* cluster could be observed for the strain ID40 when trying to validate the results by RT-qPCR. **(Fig. S2)**.

To investigate the modulation of AmpDh3 also at the protein level, the *ampDh3* gene was replaced via allelic exchange by a gene encoding AmpDh3 fused to the HiBiT fragment of the split luciferase protein[18]. This yielded the strains ID40::*ampDh3*-HiBiT, ID40Δ*ygfB*::*ampDh3*-HiBiT, and ID40Δ*ygfB*::rha-*ygfB*::*ampDh3*-HiBiT. Western blot analysis revealed that the deletion of *ygfB* increased the protein levels of AmpDh3. Complementation experiments confirmed that YgfB levels were negatively associated with that of AmpDh3 **(Fig. 1b**). It should be noted that the antibodies we used for detection of YgfB produced an unspecific band very close to YgfB but at a slightly higher molecular weight. By employing a nitrocefin assay we could furthermore show that the reduction of *ampC* expression caused by the deletion of *ygfB*

actually translated in a reduced β-lactamase activity. This effect could be reversed by the induction of *ygfB* expression via the addition of rhamnose in the strain Δ*ygfB*::rha-*ygfB* **(Fig. 1c).**

YgfB upregulates ampC by suppressing ampDh3 expression

Our previous experiments have shown that *ygfB* deletion has opposite effects on *ampC* and *ampDh3* expression. Therefore, we asked whether the increased expression levels of AmpDh3 could be causative of the reduction in *ampC* expression and consequently the AmpC protein levels in ID40Δ*ygfB*. To challenge this hypothesis, the expression of *ygfB* was induced in the strain ID40Δ*ygfB*::rha-*ygfB* by the addition of 0.1% rhamnose and mRNA transcripts of *ygfB*, *ampC* and *ampDh3* were quantified by RT-qPCR at different time points **(Fig. 2a)**. Induction of *ygfB* led to a fast decrease of *ampDh3* expression and a time-delayed increase in *ampC* mRNA expression. To confirm these findings, the strain ID40Δ*ygfB*::rha-*ygfB*::*ampDh3*-HiBiT was used for Western blot analysis. A negative association between YgfB and AmpDh3 protein levels could also be observed **(Fig. 2b)**. Taken together, these data further supported the hypothesis that YgfB might act as a suppressor of *ampDh3* expression, and that the AmpDh3 levels have to be kept low to achieve high β-lactam resistance in ID40. To challenge our assumption further, *ampDh3* and *ygfB*/*ampDh3* deletion mutants were generated and RT-qPCR was performed to analyze *ygfB*, *ampDh3* and *ampC* expression levels. As shown in **Fig. 2c**, the concurrent deletion of *ygfB* and *ampDh3* restored *ampC* expression. In contrast, *ampDh3* deletion had no impact on the expression of TUEID40_01954. This demonstrates that the suppression of *ampDh3* expression by YgfB is required to achieve high *ampC* expression in the *Pa* strain ID40.

Deletion of YgfB leads to an AmpDh3-dependent reduction in AmpR-activating anhMurNAc-peptide levels

Next, we sought to understand the connection between AmpDh3 levels and *ampC* expression. According to the current literature, *ampC* expression is regulated by the transcriptional

regulator AmpR in response to peptidoglycan turnover products and synthesis precursors[7]. AnhMurNAc-3P and anhMurNAc-5P are supposed to induce the activator function of AmpR, while UDP-MurNAc-5P induces the repressor function of AmpR in respect to AmpC β-lactamase expression[7, 8, 19]. From this we deduced that the deletion of *ygfB* might possibly indirectly change the composition of PG precursors, thereby affecting AmpC induction **(Fig. 3)**. HPLC-mass spectrometry analyses of cytosolic extracts revealed that *ygfB* deletion led to reduced levels of N-acetylglucosamine (GlcNAc)-anhMurNAc-3P as well as anhMurNAc-3P- and -5P, and increased levels of GlcNAc-anhMurNAc. Specifically, significant differences were found in the levels of these PG precursors when comparing Δ*ygfB* and Δ*ygfB*Δ*ampDh3*. No or only subtle changes in the levels of UDP-MurNAc-5P, UDP-MurNAc and anhMurNAc were found. Taken together, this means that YgfB modulates the balance between anhMurNAc-peptides and UDP-MurNAc-5P, shifting it towards an anhMurNAc-peptide-response of AmpR; i.e., the upregulation of AmpC β-lactamase. From these data it can be concluded that YgfB-mediated suppression of AmpDh3 production impacts the composition of PG precursors which in turn modulates *ampC* expression.

AmpDh3 is located in the cytoplasm

Zhang et al. demonstrated that AmpDh3 and AmpDh2 preferentially cleave long-chain peptidoglycan fragments and have much lower activity toward anhydro-muramyl derivates[13]. This led to the assumption that both AmpDh2 and AmpDh3 have to be localized in the periplasm. The finding that AmpDh3 might be translocated by a T6SS system into prey cells, however, pointed to the idea that AmpDh3 is localized in the cytosol, which however has not been demonstrated so far[15]. Therefore, we wanted to clarify where AmpDh3 is actually localized.

To assess the localization of AmpDh3, periplasmic proteins were separated from cytoplasmic proteins by spheroplasting and Western blot analysis was performed. While the periplasmic protein SurA was enriched in the periplasmic fraction, the cytoplasmic protein RpoB as well as

AmpDh3 were found predominantly in the cytoplasmic fraction, indicating that AmpDh3 is mainly located in the cytoplasm **(Fig. S3)**

YgfB suppresses AlpA-mediated AmpDh3 promoter activity

The transcriptome data suggested that YgfB suppresses *ampDh3* transcription. Previous studies by Peña et al.[17] described that both the *alpBCDE* cluster as well as the *ampDh3*-TUEID40_01954 (PA0808) operon are regulated by AlpA. AlpA seems to act as an anti-terminator and to bind to the AlpA binding element (ABE) of both the *alpBCDE* genes, as well as the *ampDh3* promoter. In their study the authors also defined a transcriptional start site (TSS) at position -413 bp upstream of the start of the CDS of *ampDh3* and a minimal promoter region between positions -469 and -409 comprising an AlpA binding element **(Fig. 4a)**. In addition, they predicted two terminator regions starting at 26 bp downstream of the ABE and at bp -178 to -137 upstream of the *ampDh3* CDS. Among the two, the terminator region in close proximity to the ABE has only a minor impact on transcription[17]. In line with this, the terminator prediction tool ARNold[20] suggests one terminator region between positions -178 to -137, corresponding to the second terminator region predicted by Peña et al.[17].

To assess the impact of YgfB on the activity of the a*mpDh3* promoter various reporter constructs were generated. This was done by fusing *ampDh3*-promoter fragments of various lengths (starting between bp -532 to bp -77 and ending at bp -1) to a reporter gene encoding the luciferase NanoLuc, using the vector pBBR1. To assess background activity, NanoLuc was cloned into pBBR1 without any promoter (0). These fragments were introduced into the conditional *ygfB* mutant ID40Δ*ygfB*::rha-*ygfB*. Subsequently, luciferase assays were performed both in the presence and in the absence of rhamnose to determine the transcriptional activity of the *ampDh3* promoter in a YgfB-dependent manner **(Fig. 4b).**

Interestingly, a promoter fragment comprising bp -77 to bp -1 was sufficient to observe YgfB-independent promoter activity. A promoter fragment comprising bp -180 to bp -1 abrogated nearly all promoter activity, which is in line with the findings of Peña et al.[17], and the existence of a terminator region. The shortest promoter fragment showing YgfB-dependent transcriptional regulation of *ampDh3* was the fragment between positions -464 and -1

comprising almost the entire suggested ABE. These data indicate that transcription can be initiated either at position -413 upstream of the *ampDh3* CDS (here referred as transcription start site 1, TSS1) or upstream of position -77 (transcription start site 2, TSS2). However, transactivation at TSS2 is not regulated by YgfB. YgfB-dependent inhibition of *ampDh3* transactivation seems to occur in the same region in which AlpA binds.

Next, the luciferase reporter plasmids 0, -77, -180 and -532 were introduced into the strains ID40, ID40Δ*ygfB*, ID40Δ*alpA* and ID40Δ*alpA*Δ*ygfB* and again the luciferase activity was measured as a proxy for the promoter activity **(Fig. 4c)**. We found that the activity of the longest promoter fragment (-532) increased upon deletion of *ygfB*. Additional deletion of *alpA* abrogated promoter activity demonstrating that AlpA is the essential factor to trigger *ampDh3* transactivation, while YgfB counteracts AlpA-induced promoter activity. The promoter fragment -180, including the terminator region, revealed no promoter activity in any of the strains. However, the promoter fragment -77 showed promoter activity independent of the presence of either AlpA or YgfB. Hence, this confirms our results obtained with the conditional *ygfB* mutant ID40Δ*ygfB*::rha-*ygfB*.

A functional PBP4 is required for basal expression of AmpDh3

Previous studies using the strain PAO1 revealed that the deletion or mutation of *dacB*, encoding the D-Ala-D-Ala-carboxypeptidase PBP4, leads to an overproduction of AmpC and results in hyperresistance[5]. Of note, the MDR *Pa* strain ID40 carries a mutation that inactivates the *dacB* gene[10, 11]. Furthermore, it was suggested that the activity of two-component system CreBC is triggered by *dacB* inactivation in response to β-lactams and affects antibiotic resistance[5]. Thus, we asked whether *dacB* inactivation and the subsequent activation of the two-component system CreBC may also influence the expression of *ampDh3* and therefore affects β-lactam resistance. For this purpose, we first investigated whether *dacB, creBC* or *ampR* inactivation contributes to the repression of *ampDh3* transactivation. To achieve this, an *ampDh3*-532-luc reporter construct was introduced into various mutants. Neither the deletion of *ampR* nor the deletion of *creBC* had an impact on the *ampDh3* promoter activity **(Fig. 5a).**

However, complementation of ID40 (naturally equipped with a non-functional *dacB*) with a functional *dacB* derived from PA14 led to a two-fold increase in *ampDh3* promoter activity after induction with rhamnose **(Fig. 5b)**. This finding indicates that PBP4 inactivation suppresses the transactivation of the *ampDh3* promoter to some extent. The impact of a non-functional *dacB* gene on *ampDh3* expression levels, however, is low in comparison to the impact of *ygfB* deletion. This suggests that the YgfB-dependent suppression of *ampDh3* is largely independent from the effects of a loss of PBP4 function.

Nevertheless, a functional PBP4 shows a higher basal transcriptional activity of the *ampDh3* promoter. To further check this, AmpDh3 production was investigated in the strain ID40::rha-*dacB*(PA14)::*ampDh3*-HiBiT. Our results show that upon induction of *dacB* expression, the AmpDh3 production was indeed ~1.5 times higher compared to uninduced cells **(Fig. 5c and d)**.

Ciprofloxacin-induced AmpDh3 production is part of the synergistic action of ciprofloxacin and β-lactam antibiotics.

DNA damage by ciprofloxacin was previously shown to increase AlpA-mediated transactivation of the *ampDh3* promoter[17]. We hypothesized that a ciprofloxacin-mediated increase in AmpDh3 production might increase the susceptibility of ID40 or ID40Δ*ygfB* toward β-lactam antibiotics.

To investigate this, ID40 and various ID40 deletion mutants were grown with or without 2.5 µg/ml ciprofloxacin (subinhibitory concentration) and MIC assays were performed after 18 h.

Ciprofloxacin showed a synergistic effect with all tested β-lactam antibiotics and led to reduced MIC values for the β-lactam antibiotics **(Table 2)**. Strains lacking *ampDh3* and grown in the presence of ciprofloxacin showed increased MIC values for meropenem, cefepime and ceftazidime indicating that ciprofloxacin-induced *ampDh3* expression slightly contributes to the synergistic effect of ciprofloxacin and β-lactam antibiotics. Ciprofloxacin breaks resistance towards all tested β-lactam antibiotics in a *ygfB* deletion mutant while the simultaneous

absence of *ampDh3* increases the resistance towards all tested antibiotics. In contrast, additional deletion of *alpA* in a *ygfB* deletion mutant increases resistance only towards some antibiotics. This suggests that deletion of AlpA does not entirely phenocopy deletion of *ampDh3* and that expression of this latter is also regulated by other factors. To monitor AmpDh3 production 18 h after treatment with or without 2.5 µg/ml ciprofloxacin, AmpDh3-HiBIT production in the strains ID40::*ampDh3*-HiBiT and Δ*ygfB*::ampDh3-HiBiT was investigated. In ID40::*ampDh3*-HiBiT, only very low levels of AmpDh3 were detected, but they were increased by the deletion of *ygfB* **(Fig. S4)**. Ciprofloxacin treatment and even more so, *ygfB* deletion strongly increased the AmpDh3 production.

Taken together, the synergistic action of ciprofloxacin and β-lactam antibiotics can to some extent be explained by ciprofloxacin-induced *ampDh3* expression, while YgfB strongly counteracts the synergistic effect of ciprofloxacin and β-lactam antibiotics.

YgfB interacts with AlpA and interferes with AlpA-DNA binding

The suppressive action of YgfB on the *ampDh3* cluster and to some extent the *alpBCDE* cluster led to the idea that YgfB may directly act on either AlpR or AlpA. To address this, the strains ID40::HA-*alpR*::*alpA*-HiBiT and ID40Δ*ygfB::*HA-*alpR*::*alpA*-HiBiT were grown for two hours without or with 32 µg/ml ciprofloxacin (8-fold MIC) and Western blot analyses were performed **(Fig. 6).**

We observed that only ciprofloxacin but not the deletion of *ygfB* reduced the levels of AlpR. Following ciprofloxacin treatment, the levels of AlpA were upregulated in ID40. However, while deletion of *ygfB* increased AlpA levels when compared to ID40, combining the deletion and ciprofloxacin treatment had no further effect on the protein levels (**Fig. 6a**).

To confirm the Western blot results, we additionally analyzed the levels of AlpA-HiBiT using the Nano-Glo HiBiT Lytic Detection System (Promega). We observed increased AlpA-HiBiT protein levels (1.6 to 2-fold) in the *ygfB* deletion mutant as assessed by measuring the luciferase activity of the fusion protein (**Fig. 6b**). Ciprofloxacin increased the levels in a similar

fashion, but once again we did not observe a synergistic effect on AlpA levels upon concurrent ciprofloxacin treatment and *ygfB* deletion.

Since YgfB seemed to influence AlpA but not AlpR, we investigated whether AlpA interacts with YgfB (**Fig. 7**). In a first attempt, recombinant GST-YgfB or GST was mixed with cell lysates of the ID40Δ*ygfB*::HA-*alpR*::*alpA*-HiBiT strain and a GST pull down assay was performed **(Fig. 7a)**. In the subsequent Western blot analysis, we could detect a band for AlpA-HiBiT when the lysates were mixed with GST-YgfB but not when mixed with GST, indicating that YgfB does interact with AlpA. To clarify whether the interaction between YgfB and AlpA is direct or indirect, we performed pulldown assays with recombinant His-MBP-AlpA or His-MBP as a bait and recombinant YgfB as a prey **(Fig. 7b)**. We observed an enrichment of YgfB when incubated with His-MBP-AlpA. This pointed to a direct interaction between AlpA and YgfB and led us to the hypothesis that the interaction of YgfB with AlpA might abrogate the ability of AlpA to bind to the *ampDh3* promoter. To test the binding of AlpA to its binding site in the *ampDh3* promoter region, electromobility shift assays (EMSAs) were performed using a probe comprising the ABE element. Addition of His-MBP-AlpA, but not the addition of His-MBP resulted in a mobility shift of the fluorophore-labeled DNA probe **(Fig. 7c and S6a)**. While the addition of bovine serum albumin to His-MBP-AlpA did not affect the complex formation between AlpA and the ABE, the addition of increasing amounts of recombinant YgfB led to a decrease in AlpA-ABE complex formation and to the formation of a DNA-protein complex with different migration. From this we concluded that YgfB not only hinders the AlpA-ABE complex formation but also directly binds to the ABE. To confirm this hypothesis, recombinant YgfB was added to the fluorophore-labeled ABE **(Fig. 7d and S6b).** We found that YgfB is in fact able to form a complex with the ABE. Competition with a non-labeled ABE probe abrogated the complex formation with the fluorophore-labeled DNA probe of both AlpA and YgfB **(Fig. 7c, d and S6)**. From these data it can be concluded that not only the interaction of YgfB with AlpA but also the binding of YgfB to the ABE interferes with the AlpA-mediated transactivation.

The role of YgfB in β-lactam resistance is conserved in other *Pa* strains

To investigate whether the prominent role of YgfB in β-lactam resistance holds true also for other MDR *P. aeruginosa* strains, *ygfB* was deleted in the clinical blood stream infection isolates ID72 and ID143 as well as in the more sensitive strains PAO1 and PA14. As depicted in **Table S1**, β-lactam resistance was also decreased in the investigated *P. aeruginosa* strains, indicating that the presence of YgfB seems to be of general importance to achieve higher resistance of *P. aeruginosa* to β-lactam antibiotics. In addition, in all tested strains, the deletion of *ygfB* led to higher *ampDh3* promoter activity **(Fig. S5a)**. However, regarding the tested strains so far it cannot be stated that lower levels of basal *ampDh3* promoter activity are a specific characteristic of more resistant strains, since the MDR strain ID40 and the sensitive strain PAO1 show similar basal *ampDh3* promoter activity **(Fig S5b)**.

Discussion

We have previously demonstrated that the deletion of *ygfB* reduces resistance against β-lactam antibiotics in an MDR *Pseudomonas aeruginosa* strain[10]. In the present study the function of YgfB in relation to β-lactam resistance was addressed. Our findings revealed that (i) YgfB-mediated suppression of the AlpA-induced production of AmpDh3 contributes to β-lactam resistance. Lack of YgfB would otherwise lead to higher AmpDh3 levels, which change the composition of peptidoglycan turnover products resulting in the AmpR-mediated reduction of *ampC* expression. (ii) YgfB interferes with the transactivating function of AlpA by direct interaction and by displacement of AlpA from the AlpA binding element. (iii) Ciprofloxacin-induced DNA damage increases the susceptibility of *Pa* to β-lactam antibiotics, an effect that is antagonized by the YgfB-mediated negative regulation of AmpDh3. (iv) Inactivation of *dacB* dampens the transcriptional activity of the *ampDh3* promoter to some extent. This may be an additional aspect of how *dacB* inactivation leads to higher resistance to β-lactam antibiotics.

Comparative transcriptome analyses of ID40 and ID40Δ*ygfB* revealed very few transcriptional changes, including the downregulation of *ampC* and the upregulation of the *ampDh3*-

TUEID40_01954 operon and the *alpBCDE* cluster. The *alpBCDE* cluster was recently described to be a potential self-lysis mechanism important for successful lung infection by *P. aeruginosa*[16]. The effect of YgfB on cell death induction is so far unclear and require follow-up studies.

P. aeruginosa possesses three paralogous amidases called AmpD, AmpDh2 and AmpDh3[13, 21]. It was already shown that loss of function mutations in *ampD* are a frequent source of MDR[4, 7]. In addition, a deletion of only *ampD* and, to a lesser extent, of either *ampDh2* or *ampDh3* was shown to increase the resistance of PAO1 to β-lactam antibiotics[22]. However, deleting both *ampD* and *ampDh3* leads to a much more pronounced resistance which can hardly be increased by additional deletion of *ampDh2*[22]. The increasing resistance associated with one or several of these amidases is also correlated with increasing levels of the cephalosporinase AmpC[22].

While the cytoplasmic protein AmpD exclusively removes the peptide from 1,6-anhydromuramyl-peptide variants, AmpDh2 and AmpDh3 show higher hydrolytic activity toward bigger peptidoglycan fragments as those found in the cell wall. AmpDh2 seems to be anchored to the inner leaflet of the outer membrane, whereas AmpDh3 was believed to be localized in the periplasm due to its higher affinity toward periplasmic substrates [13, 21]. However, both the lack of a signal peptide for the transport into the periplasm as well as the finding that AmpDh3 is a substrate for a Type VI secretion system (T6SS) in *Pa* pointed in the direction of AmpDh3 mainly acting on cytoplasmic substrates, similarly to AmpD[15]. As demonstrated in the presented study, AmpDh3 is located in the cytoplasm and seems to act redundantly with AmpD, possibly as a side effect of its main function as T6SS translocated effector as shown by Wang et al.[15].

Our data clearly indicate that YgfB increases *ampC* expression in an AmpDh3-dependent manner by decreasing of the levels of the AmpR-activating anhMurNAc-peptides[7, 8, 19]. The balance between the coeffectors UDP-MurNAc-peptides and anhMurNAc-peptides can be shifted to promote the activator function of AmpR by additional deletion of *ampDh3*. Interestingly, in the single *ygfB* deletion mutant the reduced levels of anhMurNAc-tri-

and -pentapeptide do not result in higher levels of anhMurNAc. However, in the *ygfB* deletion mutant the levels of N-Acetylglucosamine (GlcNAc)-anhMurNAc-tripeptide were decreased and the GlcNAc-anhMurNAc levels were increased. This suggests that the main target of AmpDh3 might primarily be the GlcNAc-anhMurNAc-peptides.

Thus, all these data, including the determination of the MIC values clearly demonstrate that YgfB contributes to increased β-lactam resistance by suppressing *ampDh3* expression and thereby greatly altering the anhMurNAc-peptide/UDP-MurNAc-peptide balance and the level of *ampC* expression. Changes in *ampDh3* promoter activity and antibiotic resistance due to the deletion of *ygfB* seem not only to be a property of the ID40 strain, but they could also be demonstrated for other MDR *P. aeruginosa* strains. However, the basal activity of AmpDh3 production does not seem to be directly linked to antibiotic resistance, meaning that the basal transcriptional activity of the *ampDh3* promoter cannot be used as a marker for sensitive or resistant strains.

Investigation of the role of *dacB* in YgfB-mediated suppression of *ampDh3* expression revealed that *dacB* inactivation slightly suppresses AmpDh3 production in a so far unknown and YgfB-independent manner. It can be concluded that the combined impact of YgfB and *dacB* inactivation on AmpDh3 suppression seems to be an important determinant of MDR in ID40.

A recent report showed that AlpA not only transactivates the *alpBCDE* cluster but also the *ampDh3* operon[17]. The authors proposed that AlpA binds to the ABE on the *ampDh3* promoter and then to the RNA polymerase. This binding allows the polymerase to bypass downstream terminators, resulting in *ampDh3* transcription[17]. As demonstrated in this study, deletion of *alpA* abrogates *ampDh3* transactivation of a complete *ampDh3* promoter. Our own investigations confirmed that for AlpA-positive as well as YgfB-negative regulation of the *ampDh3* promoter the same upstream stretch including the ABE is very likely required. In addition, the importance of the second terminator region could be confirmed by showing that a promoter fragment comprising bp -180 to -1 upstream of the CDS does not show transcriptional activity. However, a fragment comprising bp -77 to -1 upstream of the CDS is sufficient for high transactivation in an AlpA/YgfB-independent manner. *In silico* analysis did not reveal a putative promoter

element and at this point the second transcription initiation site is hypothetical and has to be defined in more detail.

The very specific impact of AlpA and YgfB only on the *alpBCDE* and the *ampDh3* operon led to the hypothesis that YgfB somehow interferes directly with the AlpR-AlpA axis. The model proposed by Peña et al. suggests that AlpA first binds to the promoter at the putative ABE, and then to the RNA polymerase (RNAP), allowing RNAP to bypass the intrinsic terminator positioned downstream[23]. YgfB seems to interfere with AlpA-mediated *ampDh3* expression in two different ways. First, YgfB interacts directly with AlpA which may prevent the function of AlpA to some extent, i.e. AlpA binding to the ABE. Second, YgfB binds to the ABE and replaces AlpA from its DNA binding site.

Several studies have described a synergism between ciprofloxacin and β-lactam antibiotics such as ceftazidime or aztreonam. For instance, Bosso et al. observed that in a total of 96 investigated *Pa* strains, approximately 30% showed a synergistic inhibitory effect of ciprofloxacin and aztreonam or ceftazidime[24]. For *Pa* strains which were both aztreonam and ciprofloxacin resistant, synergy was observed in 41% and resistance was broken for both antibiotics in 29% of such strains. When combining ciprofloxacin and ceftazidime, synergy was observed for 67% of the CIP/CAZ resistant strains, however, for none of the *Pa* strains resistance to both antibiotics could be broken. Various other studies reported similar results, namely that synergy between β-lactam antibiotics and ciprofloxacin can be observed for some but not all the strains of *Pa*[25, 26, 27]. ID40 is a strain resistant to CIP and most β-lactam antibiotics. In this case, subinhibitory concentrations of CIP synergize with all tested β-lactam antibiotics, breaking resistance for MEM, FEP, CAZ, ATM but not for PIP and IMP. Moreover, we could demonstrate that, at least for FEP, CAZ and ATM, the ciprofloxacin-induced expression of AmpDh3 contributes to reduced β-lactam resistance. Furthermore, the presented data show that a suppressive effect of YgfB on AlpA-mediated AmpDh3 production prevents a more profound synergistic action between CIP and β-lactam antibiotics since in the absence of *ygfB* resistance can be broken for all tested β-lactam antibiotics upon additional

treatment with CIP. Thus, the inhibitory effect of YgfB on AlpA suppresses at least partially the contribution of AmpDh3 to ciprofloxacin mediated β-lactam sensitivity. In addition, the action of YgfB may explain why CIP/β-lactam combinations are inefficient in many *Pa* strains and this highlights YgfB as an important contributor to β-lactam resistance as summarized in **Fig. 8.** Nevertheless, besides the induction of *ampDh3*, ciprofloxacin seems to re-sensitize to β-lactams via additional, as yet unknown mechanisms.

Taken together, elucidating the mechanistic basis behind the role of YgfB in β-lactam resistance, our work paves the ways for the molecular characterization of a new potential antibiotic target.

Material and Methods

Bacterial strains and culture conditions

Bacterial strains and plasmids used in this study are listed in **Supporting Table S2.** Bacteria were cultivated overnight at 37°C with shaking at 200 rpm in lysogeny broth (LB) containing suitable antibiotics if necessary. If not otherwise stated, overnight cultures were diluted 1:20 into LB broth containing suitable antibiotics or additives like L-rhamnose and grown for 3 h at 37°C and 200 rpm before sample collection for downstream analyses.

Generation of plasmids

Plasmids were generated by Gibson assembly[28]. For this purpose, vector fragments and inserts were amplified by PCR using the KAPA HIFI PCR Kit (Roche) and assembled using a Gibson Mix for 30 min at 50°C. The reaction product was transformed in *E. coli* Dh5α and selected on LB agar plates with appropriate antibiotics. Bacterial clones containing the correct plasmids were validated by sequencing (Eurofins). Primers for generation of plasmids are listed in **Table S3**.

Generation of in-frame deletion and knock-in mutants

In-frame deletion mutants were generated using the suicide plasmid pEXG2 (67) as described in Klein et al.[29] or its derivate pEXTK. In pEXTK, the *sacB* gene is replaced by a thymidine kinase gene. If pEXTK based mutator plasmids were used in the mutagenesis procedure, the positive selection to obtain a second crossover was performed by incubating merodiploidic clones for 3 h in 5 ml LB medium containing IPTG (1 mM). Subsequently, bacteria were positively selected by streaking bacteria on LB agar plates containing 200 µg/ml azidothymidine (Acros Organics) and 1 mM IPTG. Bacteria were then tested for loss of gentamicin sensitivity and mutants were verified by PCR as described previously[29]. The generated mutants and the primers used in this study are listed in **Table S2 or S3**, respectively.

Generation of complementation constructs

For complementation of ID40 with PA14 *dacB*, the coding sequences were amplified by PCR from genomic DNA of PA14 for *dacB* and assembled with the plasmid pJM220 (pUC18T-miniTn7T-gm-rhaSR-PrhaBAD)[30] by Gibson cloning. The constructed plasmids were transformed into *E.coli* SM10 λ pir and mobilized by conjugation into the mutant strains as described[31] with some modifications. A triparental mating was conducted by combining the recipient strain together with the mini-Tn7T harbouring *E.coli* SM10 λ pir strain and *E.coli* SM10 λ pir pTNS3, harbouring a Tn7 transposase. Insertion of the mini-Tn7T construct into the *att*Tn7 site was verified by PCR. Excision of the pJM220 backbone containing the Gm resistance cassette was performed by expressing Flp recombinase from a conjugative plasmid, pFLP2. Finally, sucrose resistant but gentamicin and carbenicillin sensitive colonies were verified by PCR.

RNA isolation and RT-qPCR

RNA isolation and RT-qPCR were performed as previously described [29]. The used primers are listed in **Table S3**.

Transcriptomics

The strains ID40 and ID40Δ*ygfB* were used to perform RNA sequencing and differential gene expression analysis (ID40 *vs* ID40Δ*ygfB*). The strains were subcultivated for 3 h in 5 ml LB medium. A total of four independent replicates per strain were used in the sequencing and analysis. RNA was isolated using the Quick-RNA™Fungal/Bacterial MiniprepKit (Zymo Research) according to manufacturer´s instruction. Subsequently, 15 µg RNA in 50 µl water was digested with 10 U DNAse I (Roche). The quality of the RNA was controlled by determination of the RNA Integrity Index using Agilent BioAnalyzer High Sensitivity DNA Assays. Successful depletion of DNA was controlled by qPCR and RT-qPCR for the *rpoS* and the *ygfB* genes. Next, the Zymo-Seq RiboFree total RNA Library Prep Kit (Zymo Research) was used to deplete ribosomal RNA and prepare samples for sequencing. For this step, 2 µg RNA per sample were used. Sequencing was performed with Illumina NextSeq500 (2x75 bp, MidOutput Flowcell). Mapping of sequencing reads and counting was performed using the subread package in R and the ID40 genome as a reference (https://www.ebi.ac.uk/ena/browser/view/LR700248)[32]. Differential gene expression analysis was performed using DeSeq2[33].

β-lactamase activity assay

A β-lactamase colorimetric activity assay (BioVision) based on nitrocefin turnover was performed according to manufacturers' instructions after resuspending the bacteria in 5 µl/mg β-lactamase assay buffer and diluting the supernatant of sonified bacteria 1:50 in β-lactamase assay buffer.

AmpDh3 promoter-luciferase assays

To determine the activity of the *ampDh3*-promoter, various *ampDh3*-promoter-luciferase reporter constructs such as the plasmid pBBR-ampDh3-532-nanoluc were transformed into *Pseudomonas aeruginosa* strains via electroporation according to the protocol of Choi et al.[34] (see **Table S2**).

Overnight cultures were subcultured for 3 h in 5 ml LB containing 75 µg/ml gentamicin. OD_{600} was measured and cultures were diluted to an OD_{600} of 0.2 in 1 ml LB. 50 µl were transferred into a white flat bottom 96 well plate in triplicates and 50 µl of Promega NanoGlo Luciferase assay reagent (Promega) prepared according to the manufacturer's instructions was added to the wells. The plate was then shaken for 10 min at RT and chemiluminescence was measured using a Tecan Infinite Pro 200 plate reader.

Determination of peptidoglycan catabolites in cytosolic fractions by LC-MS

P. aeruginosa ID40 parental and mutant strains were grown overnight in LB medium. The OD_{600} of overnight cultures (LB medium) was measured. 100 ml LB bacteria cultures with an initial OD_{600} of 0.05 per ml were grown for 6 h. Cells were harvested and OD_{600} measured. Bacteria were pelleted and resuspended in 20 ml 50 mM Tris-HCL buffer, pH 7.6 to a final concentration of OD_{600} = 5/ml (final OD_{600} =100). Subsequently, bacteria were centrifuged at 3,000 g for 10 min. The supernatant was discarded and the pellet frozen at -80°C. The next day, bacteria were resuspended in 400 µl water and the cultures boiled for 15 min at 95°C. Cultures were cooled down to and centrifuged at room temperature at 16,000 g for 10 min. 200 µl of the supernatant were added to 800 µl ice-cold acetone (MS grade, Sigma 34850-2.5L) to precipitate remaining proteins in the samples. Samples were then centrifuged at 4°C at 16,000 g for 10 min. The supernatant was transferred in a new tube and the cytosolic fraction was dried under vacuum for 2 h at 55°C in a Speedvac (Eppendorf). Pellets were then stored at 4°C. The dry cytosolic fractions were then dissolved in 50 µl Millipore water. 5 µl of the samples were subjected to LC-MS analysis with an UltiMate 3000 LC system (Dionex) coupled to an electrospray ionization-time of flight mass spectrometer (MicrO-TOF II; Bruker) that was operated in positive-ion mode in a mass range 180 m/z to 1,300 m/z. Metabolite separation was achieved with a Gemini C18 column (150 by 4.6 mm, 110 Å, 5 µm; Phenomenex) at 37°C with a flow rate of 0.2 ml/min in accordance with a previously described 45 min gradient program[35] with small modifications: 5 min of washing with 100% buffer A (0.1% formic acid, 0.05% ammonium formate in water), followed by a linear gradient over 30 min to 40% buffer B

(acetonitrile) and a 10 min column re-equilibration step with 100% buffer A. Peptidoglycan (PG) metabolites were shown in Data Analysis (Bruker) by extracted ion chromatograms (EICs) and the area under the curves of the respective EICs were calculated in Prism 8 (GraphPad). The theoretical m/z values of the PG metabolites investigated are 276.108 m/z for anhMurNAc, 479.187 m/z for GlcNAc-anhMurNAc, 648.272 m/z for anhMurNAc-3P, 851.352 m/z for GlcNAc-anhMurNAc-3P, 790.347 m/z for anhMurNAc-5P, 680.110 m/z for UDP-MurNAc, and 1194.349 (597.678 $^{2+}$) for UDP-MurNAc 5P.

Induction of DNA damage with ciprofloxacin

Induction of DNA-damage using ciprofloxacin was adapted from Peña et al.[17]. Overnight cultures were subcultured in LB for 3 h at 37°C and grown until exponential phase. The cultures were diluted to OD_{600} 0.5 and 32 µg/ml ciprofloxacin (Sigma-Aldrich, 8X MIC) was added to the cultures if not otherwise stated. Cultures were incubated for two hours at 37°C and harvested by centrifuging appropriate cell numbers for the desired downstream analyses.

Antibiotic susceptibility testing

For antibiotic susceptibility testing by microbroth dilution, bacterial strains were grown overnight at 37°C in LB medium. Physiological NaCl solution was inoculated to a McFarland standard of 0.5. Subsequently 62.5 µl of the suspension were transferred into 15 ml MH broth and mixed well. According to the manufacturer´s instructions, 50 µl of the suspension was transferred into each well of a microbroth dilution microtiter plate (Sensititre™ GN2F, Sensititre™ EUX2NF (Thermo Fisher Scientific)). Microtiter plates were incubated for 18 h at 37°C and OD_{600} was measured using the Tecan Infinite® 200 PRO. Bacterial strains were considered as sensitive to the respective antibiotic concentration if an OD_{600} value below 0.05 was measured. In some assays 2.5 µg/ml ciprofloxacin (subinhibitory concentration) was added.

Expression and purification of His-MBP-AlpA and His-MBP

For purification of His-MBP-AlpA and His-MBP, expression cultures of 1 liter LB medium were inoculated at an OD_{600} of 0.15 with starter cultures of *E. coli* BL21 carrying either pETM-41_AlpA or pETM-41_stop. Expression cultures were grown until an OD_{600} of 0.6-0.8 at 37°C. The cultures were then shifted to 20°C and equilibrated for 30 min. IPTG was added to a final concentration of 1 mM and expression was carried out at 20°C for 18 h. Cultures were harvested by centrifuging at 6,000 g for 10 min at 4°C.

Pellets were resuspended in 35 ml lysis buffer (50 mM Tris, 150 mM NaCl, 25 mM imidazole, pH 7.5) supplemented with lysozyme, Triton X-100, DNase and cOmplete protease inhibitor cocktail (Roche). Bacteria were lysed by sonication for 3 x 1 min on ice at 20% amplitude and 50% duty cycle. Cell debris was removed by centrifuging the lysate at 35,000 g for 1 h at 4°C. The supernatant was sterile filtered through a 0.22 µm syringe filter (Millipore) and affinity-purified in a gravity flow column using Ni^{2+}-NTA-agarose beads (Qiagen). After binding of the His-tagged proteins to the columns, columns were washed with lysis buffer and proteins were eluted using elution buffer (lysis buffer + 350 mM imidazole). Fractions were analyzed via SDS-PAGE and Coomassie staining. Elution fractions were dialyzed in 3 liter dialysis buffer (50 mM Tris, 150 mM NaCl, 20% V/V glycerol at pH 7.5) using Slide-A-Lyzer dialysis cassettes (ThermoFisher) with 20 kDa cutoff and 12-30 ml volume. Pure protein was aliquoted and stored at -80°C after snap freezing with liquid nitrogen.

Expression and purification of GST, GST-YgfB

Expression and purification were performed as above, using the strain *E. coli* BL21 carrying either carrying pGEX4T3_stop or pGEX4T3_YgfB. Differing from above, the expression was carried out at 25°C. For resuspension and lysis of the bacterial pellet, GST-A buffer (50 mM Tris, 150 mM NaCl, 1 mM DTT, pH 7.5) supplemented with lysozyme, Triton X-100, DNase and protease inhibitor was used. For purification, a GSTrap™ HP 1 ml column (Cytiva) connected to a peristaltic pump was used. After loading the column and collecting the flow through the column was washed using GST-A buffer and the protein eluted using GST-B-buffer

(50 mM Tris, 150 mM NaCl, 10 mM reduced glutathione, pH 8). After column regeneration, the flow through was loaded on the column once again and also washed and eluted. The obtained eluate fractions were pooled and dialysed against 10 liter of PBS pH 7.4 and 0.5 mM DTT using a ZelluTrans (Roth) dialysis tube with a 3.4 kDa cutoff and frozen in dialysis buffer. Analysis by SDS-PAGE and protein storage was done as described above.

Expression and purification of YgfB

Expression and purification were performed similar to as described for His-MBP and His-MBP-AlpA, using the strain *E. coli* BL21 carrying pETM-30_YgfB, however, the expression was carried out at 25°C. This purification step yielded His-GST-TEV-YgfB. Then, His-tagged TEV-protease was added to the elution fraction containing His-GST-TEV-YgfB and dialyzed in 2 l dialysis buffer (50 mM Tris, 150 mM NaCl, 1 mM DTT at pH 7.5) using a ZelluTrans (Roth) dialysis tube with a 3.4 kDa cutoff over night at 4°C.

The yielded cleavage product was purified using reverse Ni^{2+}-affinity chromatography using Ni^{2+}-NTA-agarose beads equilibrated with sterile filtered dialysis buffer and the flow through containing only YgfB was collected, aliquoted and stored as above. Fractions were analyzed via SDS-PAGE and Coomassie staining.

Generation of affinity purified antibodies against recombinant GST-YgfB

Antibodies were raised in 2 rabbits using recombinant GST-YgfB. Those obtained from one rabbit were selected for best performance against ID40, ID40Δ*ygfB* and recombinant GST-YgfB, and subsequently affinity-purified against GST-YgfB protein (Eurogentec).

Quantification of HiBiT-tagged proteins using a luciferase assay

Subcultures were harvested by centrifuging at 5,000 g for 10 min. Cell pellets were washed once by resuspending in 1 ml PBS and centrifuged at 10,000 g for 1 min. The pellet was resuspended 1 ml PBS and the OD_{600} was measured. Bacteria corresponding to an OD_{600} = 1 were harvested by centrifugation at 10,000 g for 1 min. The pelleted bacteria were

resuspended in 500 µl buffer K adapted from Dietsche et al.[36] (50 mM triethanolamine pH 7.5, 250 mM sucrose, 1 mM EDTA, 1 mM $MgCl_2$, 0.5% Triton-X 100, 10 µg/ml DNase, 2 mg/ml lysozyme, 1:100 cOmplete protease inhibitor cocktail) and incubated on ice for 30 min. For quantification of HiBiT-tagged proteins, 50 µl Nano-Glo HiBiT Lytic Reagent containing 1 µl furimazine and 2 µl recombinant LgBiT were added to 50 µl lysate in a white flat-bottom 96 well plate (Greiner) in technical triplicates. Plates were incubated for 10 min and chemiluminescence was measured using a Tecan Reader Infinite 200 Pro plate reader (500 ms integration time).

Western blot analyses from whole cell lysates

After treating bacteria according as desired, an equivalent of OD_{600} = 10 of bacteria was boiled in 2x Laemmli Sample Buffer (BioRad #1610747) supplemented with 5% 2-mercaptoethanol for 10 min at 95°C. Of the whole cell lysates, 10 µl were loaded onto a Mini Protean TGX Precast Protein gel (BioRad) with the acrylamide percentage chosen according to the protein to be detected. After separation of the proteins, they were transferred onto a nitrocellulose membrane (Amersham). HiBiT-tagged proteins were detected using the Nano-Glo HiBiT blotting system (Promega) according to the manual, while other proteins were detected via antibodies.

For this purpose, the membrane was blocked with 1x BlueBlock PF (Serva) and afterwards incubated with the primary antibody in 1x BlueBlock solution (rabbit anti-YgfB, 1:500; rabbit anti-HA-Tag, 1:1,000 (CellSignaling; HA-Tag (C29F4) Rabbit mAb #3724); mouse anti-RpoB (*Ec*), 1:1,000 (BioLegend; Anti-*E. coli* RNA Polymerase β Antibody Mouse); Rabbit anti-SurA, 1:200[29]). Next, membranes were washed three times with TBS-T (50 mM TRIS, 150 mM NaCl pH 7.4 with added 0.1% Tween-20) and afterwards incubated with the appropriate secondary antibodies (horseradish-peroxidase-conjugated goat anti-rabbit antibody 1:2,000 (Dianova; Goat F(ab')2 anti-Rabbit IgG (H+L)-HRPO, MinX none) or horse-radish-peroxidase-conjugated anti-mouse antibody, 1:2,000 (Invitrogen; Rabbit anti-Mouse IgG (H+L) Secondary Antibody, HRP)). The membranes were washed again three times using TBS-T. For detection, Clarity

Western ECL Substrate (BioRad) was added to the membrane and the signal was detected by a Fusion Solo S imager (Vilber). The anti-RpoB signal was used as loading control.

Subcellular fractionation of *Pseudomonas aeruginosa* by spheroblasting

For subcellular fractionation, a modified version of the protocol described by Wang et al. (2020) was used. *P. aeruginosa* strains were grown in LB medium overnight. The cultures were inoculated into fresh LB with the OD_{600} adjusted to 0.05 and subcultivated at 37°C with shaking to an OD_{600} = 1.5. 10 ml of each strain were harvested by centrifugation at 4,500 g for 10 min. The cell pellets were resuspended in 500 µl sucrose-EDTA solution (2.5 mM EDTA and 20% (w/v) sucrose in PBS, pH 7.3) and incubated at room temperature for 20 min. 500 µl ice-cold H_2O were added and the samples were incubated for 5 min at 4°C with gentle shaking (550 rpm). After centrifugation for 20 min at 4°C and 7,000 g, the supernatant containing all periplasmic proteins was removed and filtered through a syringe filter with 0.2 µm pore size. To obtain the cytosolic and membrane-bound proteins, the pellets were resuspended in 375 µl H_2O and 125 µl 4x Laemmli solution with 10% β-mercaptoethanol and then incubated for 10 min at 95°C.

To obtain the periplasmic proteins, 250 µl of 14.3% aqueous trichloroacetic acid solution (w/v in H_2O) were added to 1 ml of the supernatants containing the periplasmic proteins and incubated on ice for 30 min. After centrifugation for 5 min at 4°C and 14,000 g, the supernatant was discarded. The pellets were washed twice by adding 400 µl acetone, centrifuging at 14,000 g and 4°C for 5 min and discarding the acetone. The pellets were dried at 95°C for 1 min, then resuspended in 36 µl H_2O. 12 µl 4x Laemmli buffer with 10% β-mercaptoethanol were added and the samples incubated for 10 min at 95°C prior to loading on an SDS polyacrylamide gel.

GST pull-downs from cell lysates

Day cultures were inoculated at an OD_{600} of 0.1 in 500 ml of LB with overnight cultures of ID40Δ*ygfB*::*alpA*-HiBiT::HA-*alpR* and grown for 5 h at 37°C. Cultures were harvested by

centrifuging for 10 min at 6,000 g. Cell pellets were resuspended in 5 ml pulldown-buffer (50 mM Tris pH 7.5, 300 mM NaCl, 0.5% IGEPAL, 2 mM DTT) supplemented with cOmplete protease inhibitor cocktail, DNase I, lysozyme and Triton-X 100. Cells were lysed by sonification, cell debris removed by centrifugation and supernatants were used for downstream application after sterile filtration.

1 ml of recombinant GST or GST-YgfB protein at a concentration of 10 µM was incubated with 100 µl 50 % MagneGST (Promega) bead-slurry equilibrated with pulldown-buffer for 45 min at 4°C and washed two times with 500 µl pulldown-buffer. The beads were then incubated with 1 ml of cell lysate for 45 min at 4°C. After washing the beads three times with 700 µl pulldown-buffer, the bound proteins were eluted from the beads using 100 µl pulldown-buffer supplemented with 25 mM glutathione. 33 µl of 4x Laemmli buffer was added to the eluate and the samples were boiled for 10 min at 95°C. For the input samples, 10 µl of GST-tagged protein was mixed with 10 µl of cell lysate. 20 µl 4x Laemmli buffer was added and samples were boiled at 95°C for 10 minutes. Samples were analysed by SDS-PAGE and Western Blot using the Nano-Glo HiBiT blotting system (Promega).

Pulldowns using His-tagged recombinant proteins

1 ml of recombinant His-MBP-AlpA and His-MBP at a concentration of 10 µM was incubated with 100 µl MagneHis™ Ni Particles (Promega) equilibrated with pulldown-buffer (50 mM Tris pH 7.5, 25 mM imidazole, 300 mM NaCl, 0.5% IGEPAL, 2 mM DTT) for 45 min at 4°C and washed 2 times with 500 µl pulldown-buffer. 1 ml of recombinant YgfB at a concentration of 10 µM was added to the beads and incubated for 45 min at 4°C. After washing the beads three times with 700 µl pulldown-buffer, the bound proteins were eluted with 75 µl pulldown-buffer supplemented with 350 mM imidazole. 25 µl 4x Laemmli buffer were added to the eluate and the samples were boiled for 10 min at 95°C. For the input samples, 10 µl of His-tagged protein was mixed with 10 µl of rYgfB. After addition of 20 µl 4x Laemmli buffer the samples were boiled at 95°C for 10 min. Proteins were detected by SDS-PAGE and Western blot as described above.

Electromobility Shift Assays (EMSA)

For generation of the labeled probe, 5'-IRDye® 700 labeled oligonucleotides were purchased from IDT with the following sequences: 5´-CGG TGT TGC ACG CGG C**GG GAC GCT CGC GGT AGT TT**T TTC CCA TGA TCA CG-3´ and 5´-CGT GAT CAT GGG AAA **AAA CTA CCG CGA GCG TCC C**GC CGC GTG CAA CAC CG-3´. The AlpA binding element is shown in bold letters. The oligonucleotides were annealed by mixing them in equimolar amounts in duplexing buffer (100 mM Potassium Acetate; 30 mM HEPES, pH 7.5) and heating to 100°C for 5 min in a PCR cycler. The cycler was then turned off and the samples were allowed to cool to room temperature while still inside the block. The annealed product was then diluted with water to 6.25 nM for EMSA experiments. For generation of the competitor, the same procedure was performed with unlabeled oligonucleotides purchased from Sigma-Aldrich but the product was diluted to 20 µM.

For EMSAs fluorophore labeled DNA probes at a concentration of 0.3125 nM were incubated for 30 min at 20°C in 20 µl reaction mix (Licor Odysee EMSA Kit) containing 33.4 mM Tris, 70.2 mM NaCl, 12.5 mM NaOAc, 3.75 mM HEPES, 50 mM KCl, 3.5 mM DTT, 0.25% Tween-20 and 1 µg poly(dI-dC) with proteins or competitors at the indicated concentrations. For resolving the reactions, 4% polyacrylamide gels containing 30% triethylene glycol were cast (For two gels: 2 ml ROTIPHORESE®Gel 30 37.5:1 (Roth), 4.5 ml triethylene glycol (Sigma-Aldrich), 1.5 ml 5x TBE-buffer, 7 ml ddH2O, 15 µl TEMED, 75 µl 10% APS). The gels were preequilibrated for 30 minutes at 130 V in 0.5x TBE-buffer. Samples with added 10x orange dye were then loaded onto the gel at 4°C and the voltage set to 300 V until the samples entered the gel completely. The voltage was then turned down to 130 V and the gel was run until the migration front reached the end of the gel. The gels were imaged using the Licor Odyssey imaging system using the 700 nm channel.

Statistics

Statistics were performed using GraphPad Prism 9.12 software as described for each experiment in the table or figure legends.

Data availability

Transcriptomic data is available on the server of the National Library of Medicine under the accession number PRJNA835697 Reviewer link: https://dataview.ncbi.nlm.nih.gov/object/PRJNA835697?reviewer=fe3gcngqnecij22uk4lm999mte. Genomic DNA sequence of ID40 is available under https://www.ebi.ac.uk/ena/browser/view/LR700248. Primary data are available from the corresponding author upon request.

Acknowledgments

This work was financed by Grants from the Deutsche Forschungsgemeinschaft (DFG) (BO 1527/4-1) to EB/MS; the German Center of Infection Research (DZIF) to MS and the DFG Cluster of Excellence EXC2124 'Controlling Microbes to Fight Infection' (CMFI) to CM/EB. LM was supported by the intramural IZKF program of the Medical Faculty at the University of Tübingen. We thank Libera Lo Presti for the critical reading of the manuscript, fruitful comments and great corrections.

Contribution of authors:

Study design EB, MS, FR, OE, CM, MB; manuscript and figures by EB, MS, FR, OE, MB, VE, CM; transcriptomics AA, CE, EW, EB; analysis of PG precursors by MB, EB, CM; generation of mutants by EB, EW, FS, KK, NW, OE, LM, VE, MS; protein purification and antibody generation by FR, OE, FS, KK; protein-protein interaction by OE, FS; EMSAs by OE, Western blots by OE, FS, NW; localization of AmpDh3 by VE; *ampDh3* promoter analysis by EB, EW, LM, NW; Quantification of HiBiT tagged proteins by EB, OE; in silico analysis FR; antibiotic resistance and β-lactamase activity by EW, NW, OE, LM, MS.

Figures

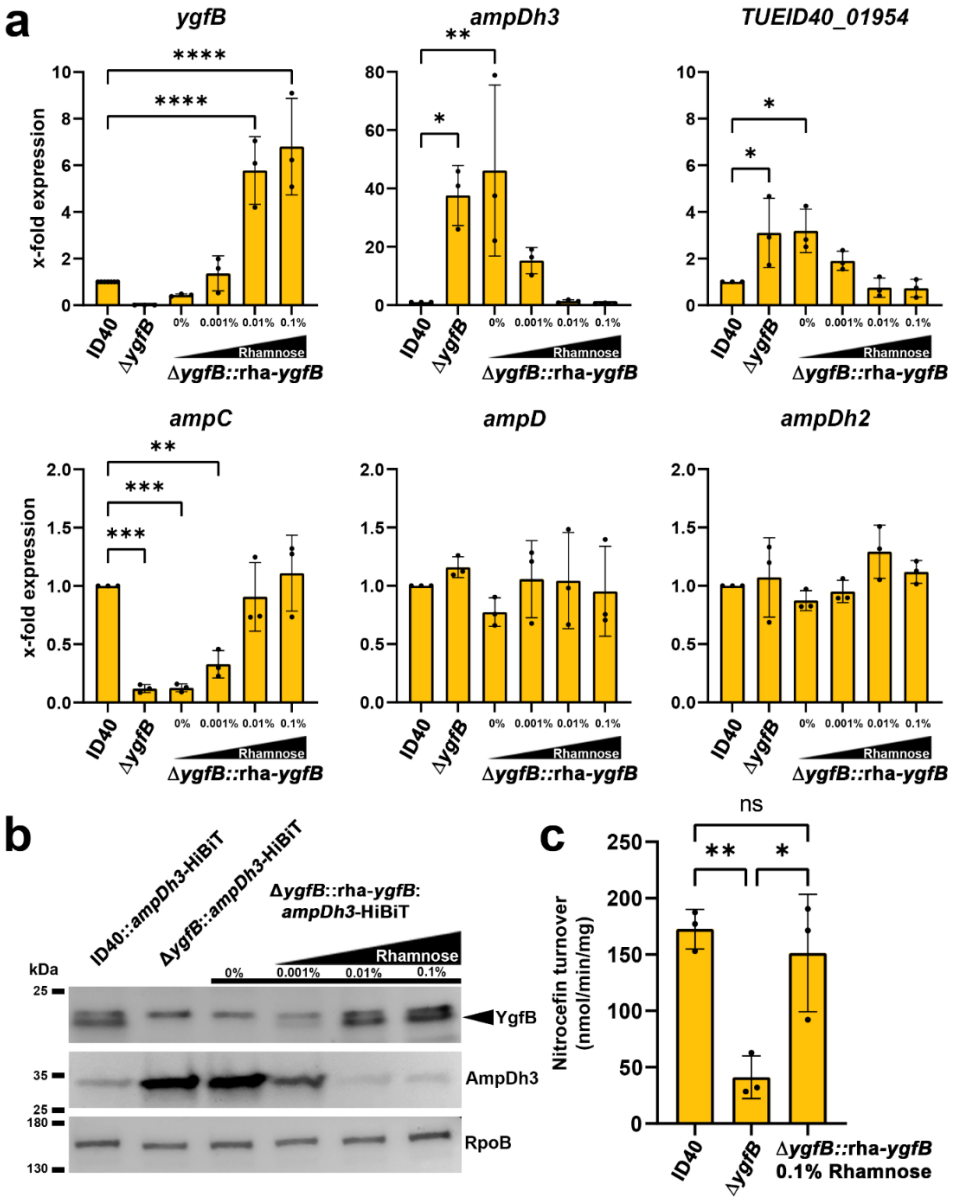

Fig.1: Validation of transcriptomic data. (a) RNA was isolated from the indicated strains and RT-qPCR performed. Data depict the mean and SD of the x-fold difference in mRNA expression compared to ID40 of *n*=3 individual experiments. Asterisks depict significant differences (*p<0.05, **p<0.01, ****p<0.001; one-way ANOVA, Dunnett's multiple comparison comparing to ID40). (b) Whole cell lysates of the indicated strains were used for SDS-PAGE and Western blots. As primary antibodies, anti-YgfB or as a loading control anti-RpoB antibodies and as secondary antibody anti-IgG-HRP antibodies were used and detection was done using ECL. For determination of AmpDh3, recombinant LgBiT was used. LgBiT binds to HiBiT resulting in a functional luciferase. The cleavage of the substrate furimazine leads to detectable chemiluminescence. Data are representative of three independent experiments (c) Whole cell lysates from the indicated strains were used to determine β-lactamase activity using a nitrocefin assay. Data depict the mean and SD of nitrocefin turnover for *n*=3 individual experiments. Asterisks depict significant differences (ns p>0.05, *p<0.05, **p<0.01, ****p<0.001; one-way ANOVA, Tukey's multiple comparisons).

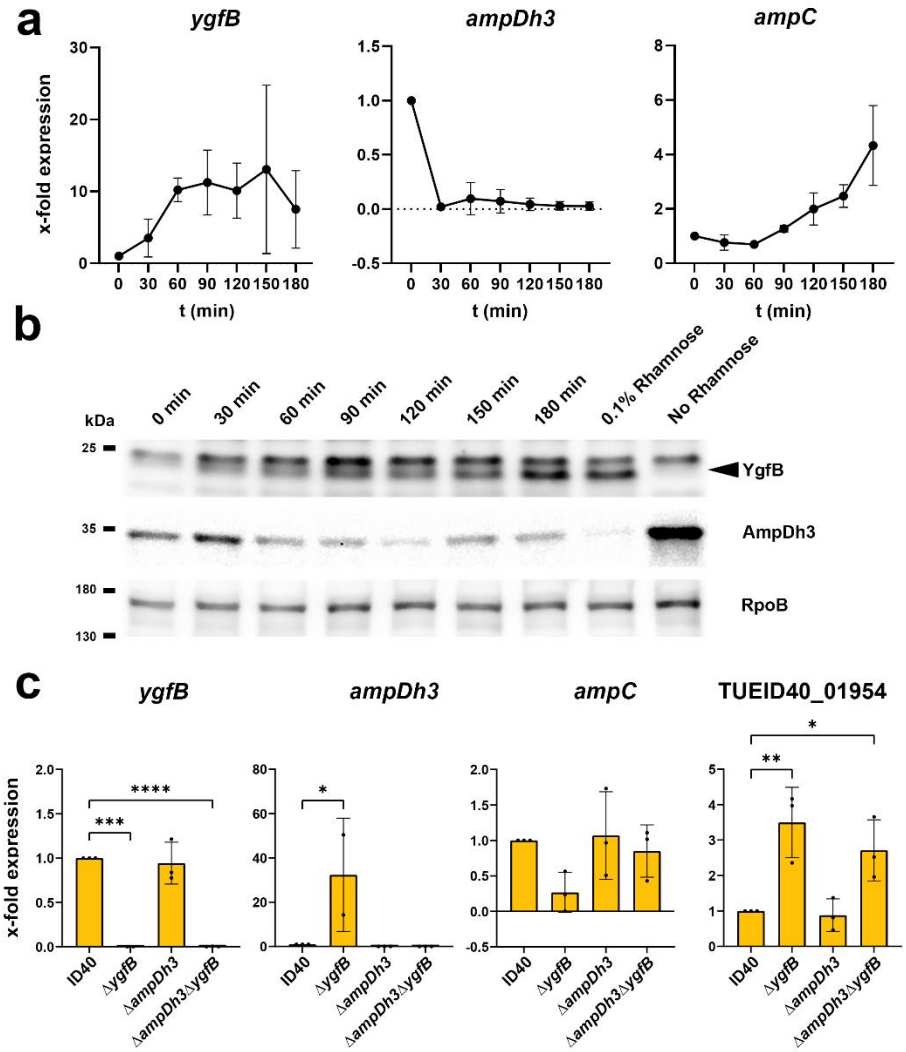

Fig.2: Relationship between YgfB, AmpDh3 and AmpC. (a) The expression of *ygfB* in ID40Δ*ygfB*::rha-*ygfB* was induced with 0.1% rhamnose at time point zero and RNA was isolated at various time points of growth in LB medium for further use in RT-qPCRs. Data depict the mean and SD of x-fold expression compared to ID40 0 min of *n*=3 independent experiments (b) The expression of *ygfB* in ID40Δ*ygfB*::rha-*ygfB*::*ampDh3*-HiBiT was induced with 0.1% rhamnose at time point zero and samples were taken from the growing culture in LB medium at the indicated time points. Then, whole cell lysates were prepared and used for SDS-PAGE and Western blots. The 0.1% condition depicts a strain grown under constant rhamnose supplementation. As primary antibodies, anti-YgfB or anti-RpoB antibodies and as secondary antibody anti-IgG-HRP antibodies were used and detection was done using ECL. For determination of AmpDh3, recombinant LgBiT was used. LgBiT binds to HiBiT resulting in a functional luciferase. The cleavage of the substrate furimazine leads to detectable chemiluminescence. Data are representative of three independent experiments. (c) *Pa* strains as indicated were grown for 3 h in LB. RNA was isolated and used for RT-qPCR. Data depict mean and SD of x-fold mRNA expression compared to ID40 of *n*=2-3 independent experiments. Asterisks indicate significant differences compared to ID40 (*p<0.05, **p<0.01, ***p<0.001, ****p<0.0001; one-way ANOVA, Dunnett's multiple comparisons comparing to ID40).

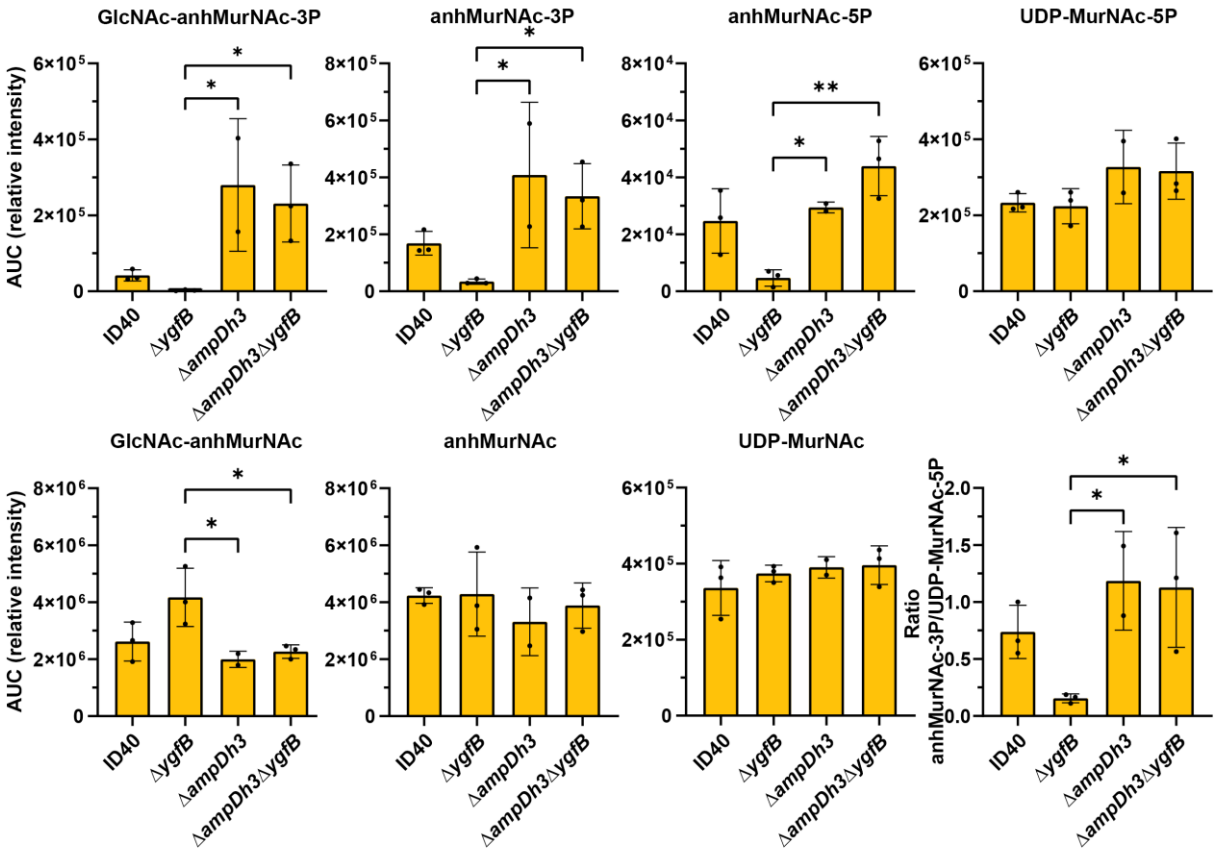

Fig.3: Impact of YgfB and AmpDh3 on the composition of peptidoglycan precursors. The indicated *Pa* strains were grown for 6 h in LB medium, cytosolic extracts were generated and analyzed by HPLC-mass spectrometry. The graphs depict the mean and SD of the area under curve (AUC) of the peaks obtained for various catabolites of *n*=2-3 independent experiments. In addition, the ratio between anhMurNAc-3-P and UDP-MurNac-5-P is shown. Asterisks indicate significant differences between Δ*ygfB* and all other groups (*p<0.05, **p<0.01; one-way ANOVA, Dunnett's multiple comparisons comparing to Δ*ygfB*).

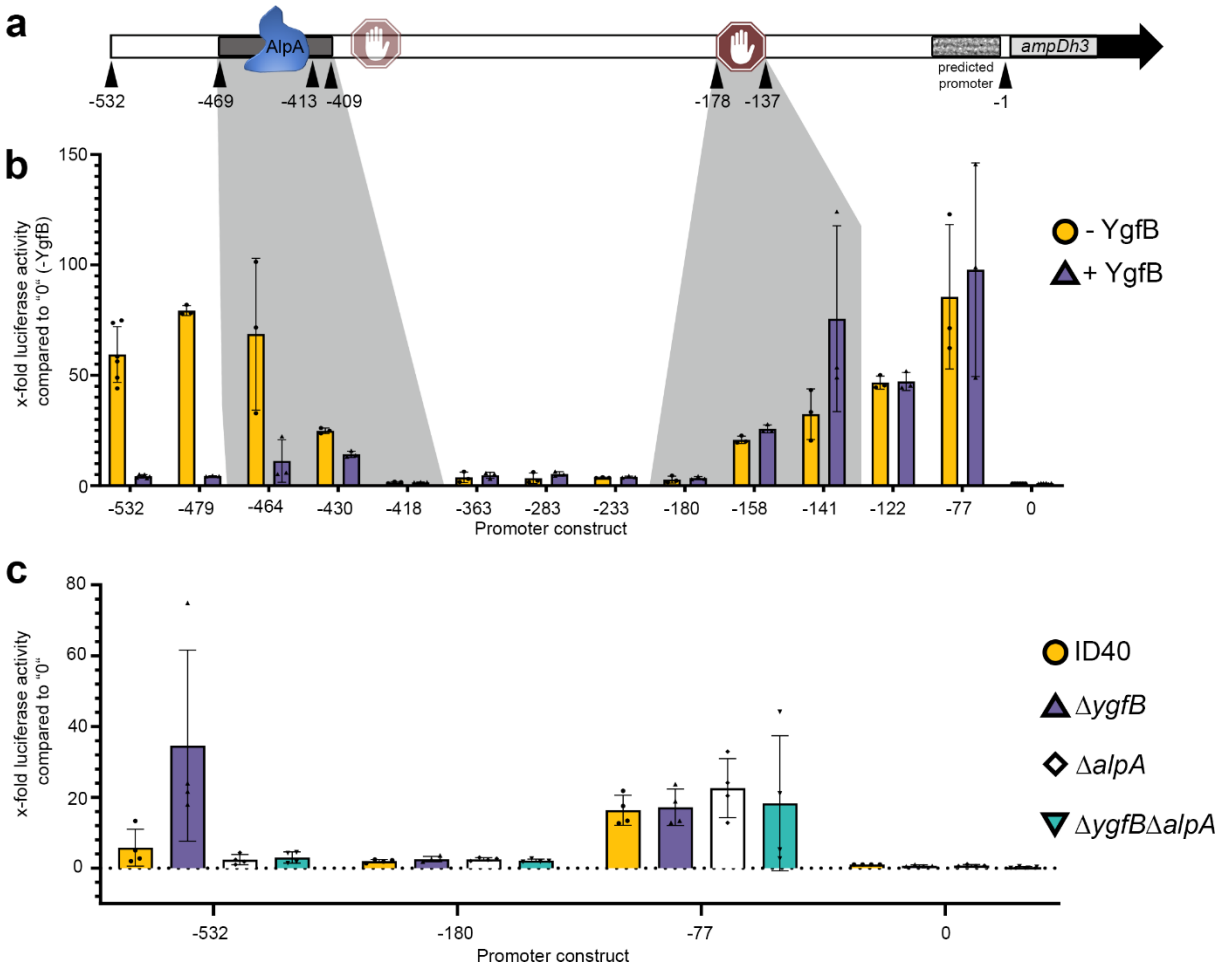

Fig.4: Analysis of the *ampDh3* promoter. (a) Schematic view of the putative *ampDh3* promoter. Numbers below depict the base pairs counted upstream of the coding sequence (CDS). The black bar in which blue AlpA is depicted marks the AlpA binding element (ABE) as defined by Peña et al[17]. Stop symbols mark terminator regions as predicted. (b and c) Luciferase assays were performed to measure transcriptional activity using *ampDh3* promoter fragments of various lengths fused to the coding sequence of NanoLuc. Data depict the mean and SD of the x-fold luciferase activity of 0-luc compared to all other fragments of *n*=3, 6 for (b) and *n*=4 for (c) independent experiments. In (b), the strain ID40Δ*ygfB*::rha-*ygfB* with (blue triangle) and without (yellow circle) 0.1% rhamnose and in (c) the strains ID40, Δ*ygfB*, Δ*alpA,* Δ*ygfB*Δ*alpA* were used as indicated. The depicted strains carry the indicated pBBR plasmids in which the expression of NanoLuc is under the control of fragments of different length of the *ampDh3* promoter. For instance, -532 is the abbreviation for a pBBR plasmid containing an *ampDh3* promoter fragment comprising the region -532 to -1 bp upstream of the CDS of Nanoluc.

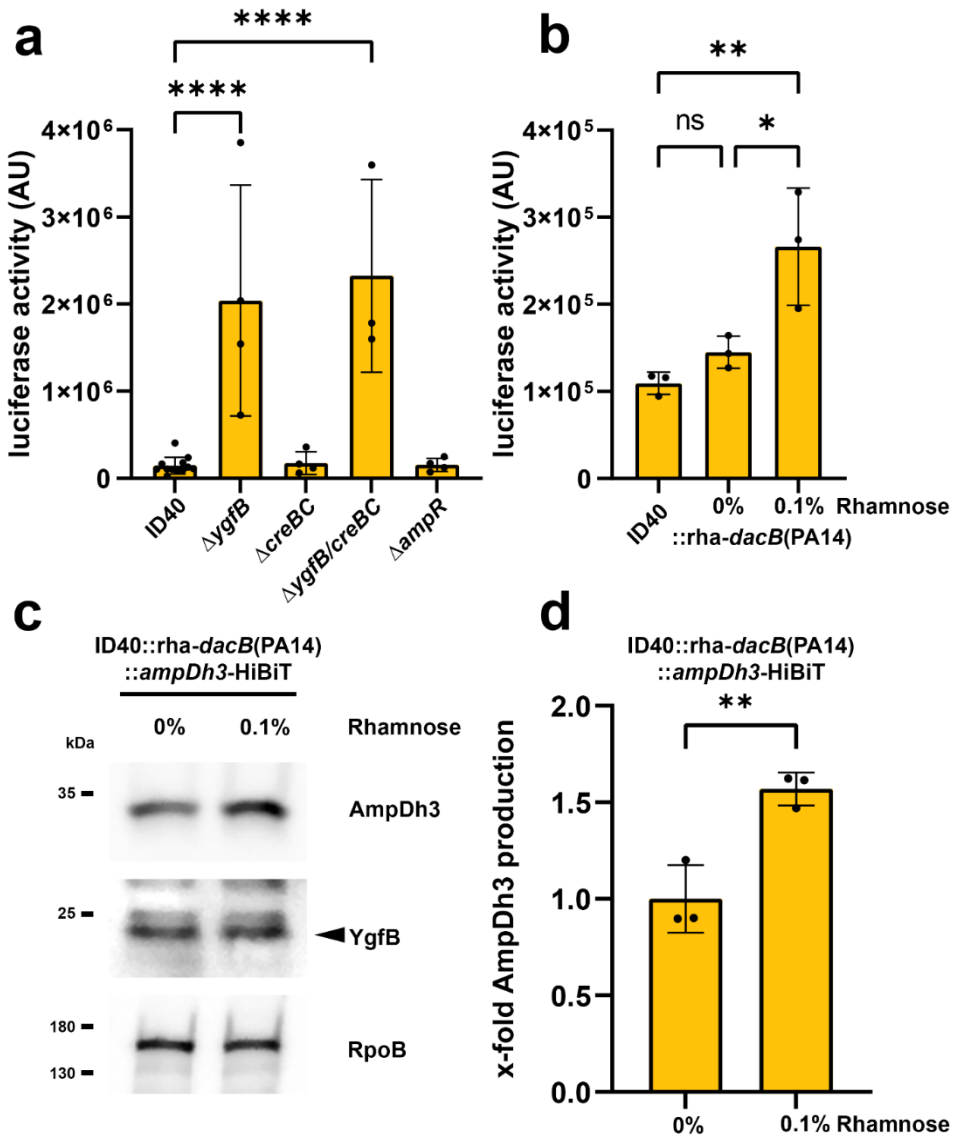

Fig. 5: Interrelationship between *creBC*, *dacB* and *ampDh3*. (a and b) Luciferase reporter assays using the indicated strains harboring the reporter construct *ampDh3*-532-luc comprising the *ampDh3* promoter fragment between position -532 and -1 upstream of the CDS of Nanoluc. Data depict the mean and SD of luciferase activity of *n*=12, 4, 4, 3, 4 for (a) and *n*=3 for (b) independent experiments. Asterisks in (a) indicate significant differences compared to ID40 (****p<0.0001; one-way ANOVA, Dunnett's multiple comparisons comparing to ID40) and in (b) compared between all conditions (ns p>0.05, *p<0.05, **p<0.01; one-way ANOVA, Tukey's multiple comparisons).
(c) ID40::rha-*dacB* (PA14) was grown for 3 h without or with 0.1% rhamnose to induce the expression of *dacB* of PA14 in LB medium at 37°C. Whole cell lysates were used to perform SDS-PAGE and Western blot transfer. As primary antibodies anti-YgfB or anti-RpoB antibodies and as secondary antibodies anti-IgG-HRP antibodies were used and detection was done using ECL. AmpDh3-HiBiT was detected by incubating the membrane with LgBiT and furimazine. Data are representative for three independent experiments. (d) Bacteria were harvested, lysed and subsequently luciferase activity of AmpDh3-HiBiT was measured as described in material and methods. Data depict the mean and SD of the luciferase activity of *n*=3 independent experiments. Asterisks indicate significant differences (p**<0.01; unpaired, two-tailed t-test).

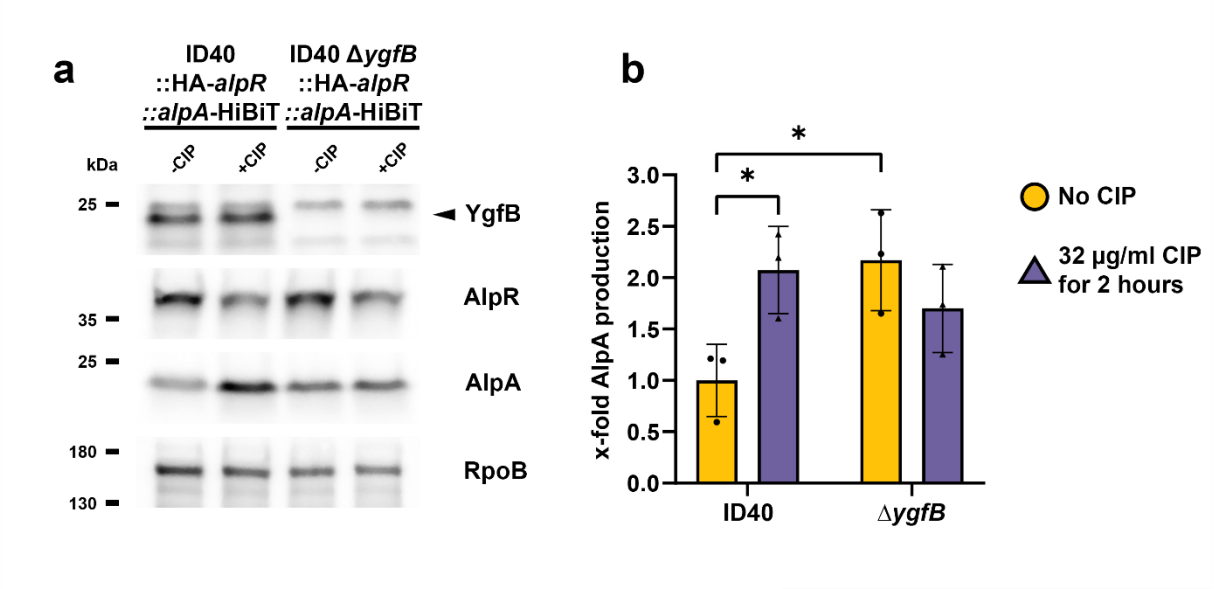

Fig.6: Modulation of AlpR and AlpA production by YgfB and ciprofloxacin (CIP). (a) Whole cell lysates of the indicated strains were used for Western blot analyses. As primary antibodies, anti-HA, anti-YgfB or anti-RpoB antibodies and as secondary antibody anti-IgG-HRP antibodies were used and detection was done using ECL. For detection of AlpA-HiBiT or AmpDh3-HiBiT, recombinant LgBiT was used. LgBiT binds to HiBiT resulting in a functional luciferase. The cleavage of the substrate furimazine leads to detectable chemiluminescence. Data are representative of three independent experiments (b) Quantification of AlpA by measuring luciferase activity of AlpA-HiBiT in lysed cell extracts. Data depict mean and SD of x-fold luciferase activity compared to ID40 WT for *n*=3 independent experiments. Asterisks indicate significant differences compared to ID40 -CIP (*p<0.05; two-way ANOVA, Šídák's multiple comparisons comparing to ID40 -CIP).

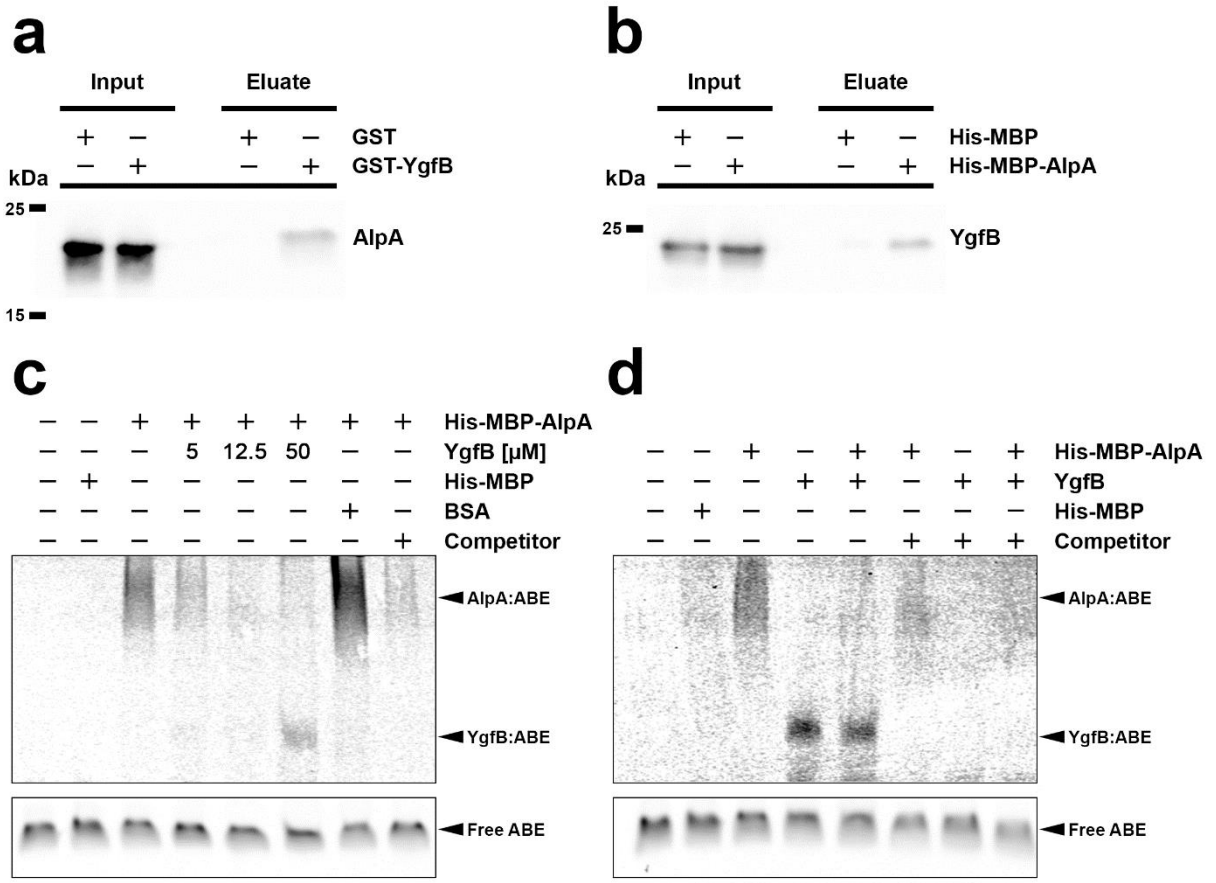

Fig.7: Interaction of AlpA with YgfB or *ampDh3* promoter. Pulldowns were performed using (a) recombinant GST-YgfB or GST as a bait and cell lysates of ID40Δ*ygfB*::*alpA*-HiBiT::HA-*alpR* as the prey and (b) recombinant His-MBP or His-MBP-AlpA as a bait and recombinant YgfB as the prey. Shown are Western blots using either LgBiT or anti-YgfB antibodies for detection. (c) and (d) EMSAs using 0.3125 nM IRDye700-labeled AlpA binding element incubated with the indicated proteins or non-labeled AlpA binding element (Competitor). Concentrations used: His-MBP-AlpA and His-MBP 1.25 µM; YgfB 5-50 µM (c) and 50 µM (d); bovine serum albumin (BSA) 50 µM and competitor 5 µM. Detection of IRDye700 was performed using the Licor Odyssey detection system. Of note, to obtain a higher dynamic range the free dsDNA and the shifted DNA-protein complexes were recorded separately. Full image is provided in **Fig. S6**).

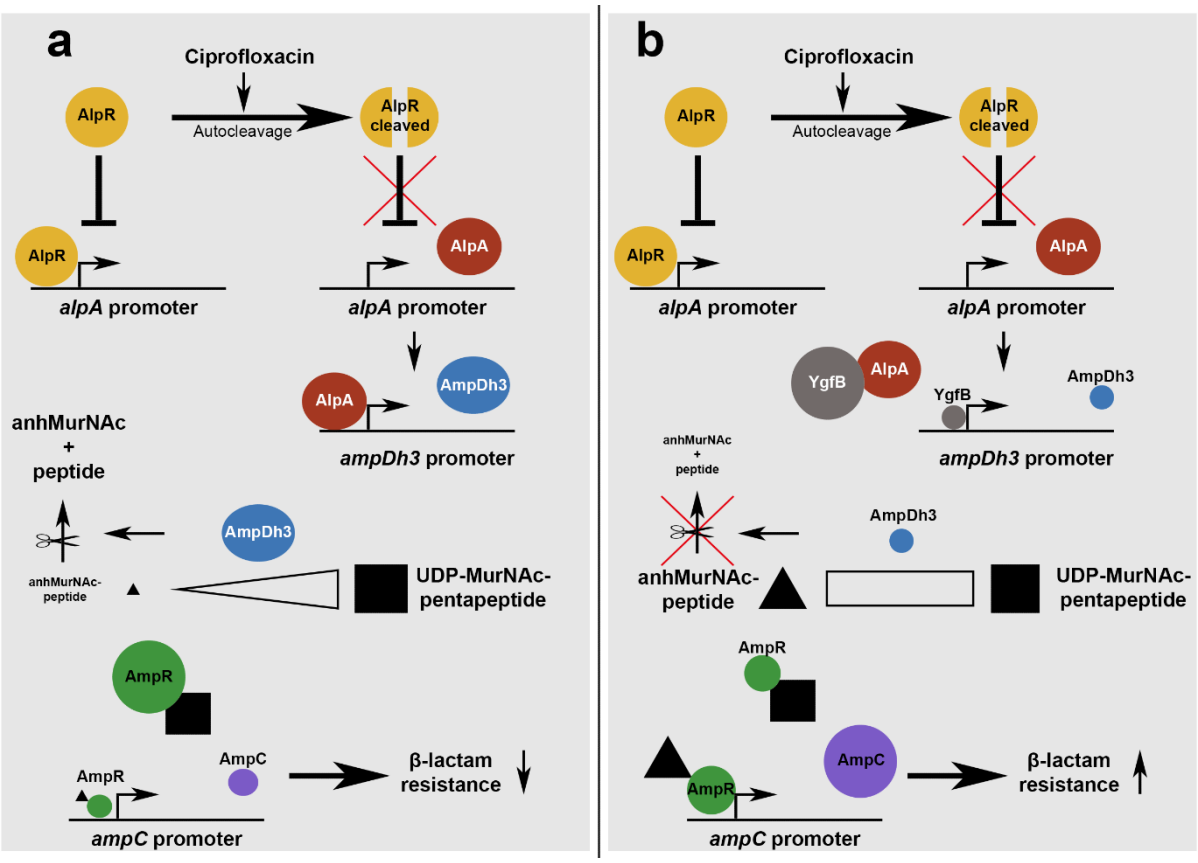

Fig.8: Ciprofloxacin induced signaling pathway leading to modulation of *ampC* expression. (a) Ciprofloxacin triggers DNA damage which promotes autocleavage of AlpR and as a consequence, the derepression of the *alpA* promoter. AlpA acts as an antiterminator of *ampDh3* expression increasing AmpDh3 production. AmpDh3 cleaves anhMurNAc peptides which changes the balance of the AmpR-activator upon binding anhMurNAc-peptides and the AmpR-repressor upon binding UDP-MurNAc-pentapeptides in favor of AmpR-mediated repression of its target promoters. This leads to reduced *ampC* expression and decreased β-lactam resistance.

(b) YgfB directly interacts with AlpA and blocks binding of AlpA to the *ampD3* promoter. In addition, YgfB can directly bind to the AlpA-binding element and prevents AlpA binding. Thereby, AlpA's antiterminator function is inhibited and *ampDh3* expression dampened. Reduced levels of AmpDh3 in the cytosol change the balance of AmpR-activating anhMurNAc-peptides and AmpR-repressing UDP-MurNAc-pentapeptides in favor of AmpR-mediated activation of its target promoters. This enhances AmpC production and leads to increased β-lactam resistance.

Table 1: Transcriptomic analyses. Complete list of genes with significant changes in mRNA expression due to *ygfB* deletion.

Gene ID (ID40)	**PAO1 orthologue**	**Product**	**Function**	**Δ*ygfB* vs WT**	
				Log2-fold change	Adjusted p value
TUEID40_03245	PA5225	*ygfB*	unknown	-3.876	0
TUEID40_04486	PA4110	*ampC*	β-lactamase	-2.303	1.23E-7
TUEID40_01840	PA0908	*alpB*	Self-lysis pathway	2.053	0.000771
TUEID40_01839	PA0909	*alpC*	Self-lysis pathway	2.504	0.0000128
TUEID40_01838	PA0910	*alpD*	Self-lysis pathway	1.527	0.0179
TUEID40_01837	PA0911	*alpE*	Self-lysis pathway	1.367	0.0374
TUEID40_01945	PA0817	-	Glyoxalase-like domain protein	1.9	0.0000337
TUEID40_01955	PA0807	*ampDh3*	Amidase	5.395	3.446E-11
TUEID40_01954	PA0808	-	Immunity protein	2.504	1.87E-62

Table 2: Modulation of β-lactam resistance by ciprofloxacin. Minimal inhibitory concentration (MIC) values (in mg/l) for the indicated strains treated with or without 2.5 µg/ml ciprofloxacin. MEM meropenem, IMP imipenem, FEP cefepime, CAZ ceftazidime, PIP piperacillin, TZP tazobactam/piperacillin, AZT aztreonam, CIP ciprofloxacin. Green: reduced MIC compared to WT, Green bold and green coloured field: resistance is broken, Red: MIC value higher than WT.

	MEM	IMP	FEP	CAZ	PIP	TZP	AZT	CIP
MIC S≤	**2**	**4**	**8**	**8**	**16**	**16**	**16**	**0.5**
MIC R>	**8**	**4**	**8**	**8**	**16**	**16**	**16**	**0.5**
ID40WT	8-16	64	16-32	32->32	128	128	>32	>4
ID40Δ*ampDh3*	8	64	32	>32	128	>128	>32	>4
ID40Δ*alpA*	8	64	32	>32	128	128	32	>4
ID40WT +CIP	**2**	32	**4**	**8**	32	32	**4**	>4
ID40Δ*ampDh3* +CIP	4	32	**8**	16	32	**16**	**4**	>4
ID40Δ*alpA*+CIP	**2**	32	**<1**	**8**	32	16-32	**4**	>4
ID40Δ*ygfB*	4	8-16	8-16	16-32	32-64	32	**16**	>4
ID40Δ*ampDh3*Δ*ygfB*	8	64	32	>32	>128	>128	32	>4
ID40Δ*alpA*Δ*ygfB*	8	32	16	>32	>128	128	32	>4
ID40Δ*ygfB* +CIP	**1-2**	**4**	**4**	**2**	**<16**	**<4**	**2**	>4
ID40Δ*ampDh3*Δ*ygfB* +CIP	2-4	32	**8**	8-16	64	16-32	**4**	>4
ID40Δ*alpA*Δ*ygfB* +CIP	**1-2**	32	**<1**	**8**	32	16-32	**4**	>4

References

1. Yoshimura F, Nikaido H. Permeability of *Pseudomonas aeruginosa* outer membrane to hydrophilic solutes. *J Bacteriol* **152**, 636-642 (1982).

2. Strateva T, Yordanov D. *Pseudomonas aeruginosa* - a phenomenon of bacterial resistance. *Journal of medical microbiology* **58**, 1133-1148 (2009).

3. Schmidtke AJ, Hanson ND. Role of ampD homologs in overproduction of AmpC in clinical isolates of *Pseudomonas aeruginosa*. *Antimicrob Agents Chemother* **52**, 3922-3927 (2008).

4. Tam VH*, et al.* Prevalence of AmpC over-expression in bloodstream isolates of *Pseudomonas aeruginosa*. *Clin Microbiol Infect* **13**, 413-418 (2007).

5. Moya B*, et al.* Beta-lactam resistance response triggered by inactivation of a nonessential penicillin-binding protein. *PLoS pathogens* **5**, e1000353 (2009).

6. Sanders CC, Sanders WE, Jr. Type I beta-lactamases of gram-negative bacteria: interactions with beta-lactam antibiotics. *J Infect Dis* **154**, 792-800 (1986).

7. Torrens G*, et al.* Regulation of AmpC-Driven beta-Lactam Resistance in *Pseudomonas aeruginosa*: Different Pathways, Different Signaling. *mSystems* **4**, (2019).

8. Jacobs C, Frere JM, Normark S. Cytosolic intermediates for cell wall biosynthesis and degradation control inducible beta-lactam resistance in gram-negative bacteria. *Cell* **88**, 823-832 (1997).

9. Hanson ND, Sanders CC. Regulation of inducible AmpC beta-lactamase expression among Enterobacteriaceae. *Curr Pharm Des* **5**, 881-894 (1999).

10. Sonnabend MS*, et al.* Identification of Drug Resistance Determinants in a Clinical Isolate of *Pseudomonas aeruginosa* by High-Density Transposon Mutagenesis. *Antimicrob Agents Chemother* **64**, (2020).

11. Willmann M*, et al.* Multi-omics approach identifies novel pathogen-derived prognostic biomarkers in patients with *Pseudomonas aeruginosa* bloodstream infection. *bioRxiv*, 1-35 (2018).

12. Galkin A, Sarikaya E, Lehmann C, Howard A, Herzberg O. X-ray structure of HI0817 from *Haemophilus influenzae*: protein of unknown function with a novel fold. *Proteins* **57**, 874-877 (2004).

13. Zhang W, Lee M, Hesek D, Lastochkin E, Boggess B, Mobashery S. Reactions of the three AmpD enzymes of *Pseudomonas aeruginosa*. *Journal of the American Chemical Society* **135**, 4950-4953 (2013).

14. Moya B, Juan C, Alberti S, Perez JL, Oliver A. Benefit of having multiple ampD genes for acquiring beta-lactam resistance without losing fitness and virulence in *Pseudomonas aeruginosa*. *Antimicrob Agents Chemother* **52**, 3694-3700 (2008).

15. Wang T*, et al.* A type VI secretion system delivers a cell wall amidase to target bacterial competitors. *Mol Microbiol*, (2020).

16. McFarland KA*, et al.* A self-lysis pathway that enhances the virulence of a pathogenic bacterium. *Proc Natl Acad Sci U S A* **112**, 8433-8438 (2015).

17. Peña JM*, et al.* Control of a programmed cell death pathway in Pseudomonas aeruginosa by an antiterminator. *Nat Commun* **12**, 1702 (2021).

18. Westerhausen S*, et al.* A NanoLuc luciferase-based assay enabling the real-time analysis of protein secretion and injection by bacterial type III secretion systems. *Mol Microbiol* **113**, 1240-1254 (2020).

19. Jacobs C, Huang LJ, Bartowsky E, Normark S, Park JT. Bacterial cell wall recycling provides cytosolic muropeptides as effectors for beta-lactamase induction. *The EMBO journal* **13**, 4684-4694 (1994).

20. Naville M, Ghuillot-Gaudeffroy A, Marchais A, Gautheret D. ARNold: a web tool for the prediction of Rho-independent transcription terminators. *RNA Biol* **8**, 11-13 (2011).

21. Rivera I, Molina R, Lee M, Mobashery S, Hermoso JA. Orthologous and Paralogous AmpD Peptidoglycan Amidases from Gram-Negative Bacteria. *Microb Drug Resist* **22**, 470-476 (2016).

22. Juan C, Moya B, Perez JL, Oliver A. Stepwise upregulation of the *Pseudomonas aeruginos*a chromosomal cephalosporinase conferring high-level beta-lactam resistance involves three AmpD homologues. *Antimicrob Agents Chemother* **50**, 1780-1787 (2006).

23. Cabot G*, et al.* Overexpression of AmpC and efflux pumps in *Pseudomonas aeruginosa* isolates from bloodstream infections: prevalence and impact on resistance in a Spanish multicenter study. *Antimicrob Agents Chemother* **55**, 1906-1911 (2011).

24. Bosso JA, Saxon BA, Matsen JM. In vitro activities of combinations of aztreonam, ciprofloxacin, and ceftazidime against clinical isolates of Pseudomonas aeruginosa and Pseudomonas cepacia from patients with cystic fibrosis. *Antimicrob Agents Chemother* **34**, 487-488 (1990).

25. Rees VE*, et al.* Meropenem Combined with Ciprofloxacin Combats Hypermutable Pseudomonas aeruginosa from Respiratory Infections of Cystic Fibrosis Patients. *Antimicrob Agents Chemother* **62**, (2018).

26. Bustamante CI, Wharton RC, Wade JC. In vitro activity of ciprofloxacin in combination with ceftazidime, aztreonam, and azlocillin against multiresistant isolates of Pseudomonas aeruginosa. *Antimicrob Agents Chemother* **34**, 1814-1815 (1990).

27. Kanellakopoulou K, Sarafis P, Galani I, Giamarellou H, Giamarellos-Bourboulis EJ. In vitro synergism of beta-lactams with ciprofloxacin and moxifloxacin against genetically distinct multidrug-resistant isolates of Pseudomonas aeruginosa. *International journal of antimicrobial agents* **32**, 33-39 (2008).

28. Gibson DG, Young L, Chuang RY, Venter JC, Hutchison CA, 3rd, Smith HO. Enzymatic assembly of DNA molecules up to several hundred kilobases. *Nature methods* **6**, 343-345 (2009).

29. Klein K*, et al.* Deprivation of the Periplasmic Chaperone SurA Reduces Virulence and Restores Antibiotic Susceptibility of Multidrug-Resistant *Pseudomonas aeruginosa*. *Frontiers in microbiology* **10**, 1-17 (2019).

30. Meisner J, Goldberg JB. The *Escherichia coli* rhaSR-PrhaBAD Inducible Promoter System Allows Tightly Controlled Gene Expression over a Wide Range in *Pseudomonas aeruginosa*. *Appl Environ Microbiol* **82**, 6715-6727 (2016).

31. Choi KH, Schweizer HP. mini-Tn7 insertion in bacteria with single attTn7 sites: example *Pseudomonas aeruginosa*. *Nat Protoc* **1**, 153-161 (2006).

32. Liao Y, Smyth GK, Shi W. The R package Rsubread is easier, faster, cheaper and better for alignment and quantification of RNA sequencing reads. *Nucleic Acids Res* **47**, e47 (2019).

33. Love MI, Huber W, Anders S. Moderated estimation of fold change and dispersion for RNA-seq data with DESeq2. *Genome Biol* **15**, 550 (2014).

34. Choi KH, Kumar A, Schweizer HP. A 10-min method for preparation of highly electrocompetent Pseudomonas aeruginosa cells: application for DNA fragment transfer between chromosomes and plasmid transformation. *Journal of microbiological methods* **64**, 391-397 (2006).

35. Gisin J, Schneider A, Nagele B, Borisova M, Mayer C. A cell wall recycling shortcut that bypasses peptidoglycan de novo biosynthesis. *Nat Chem Biol* **9**, 491-493 (2013).

36. Dietsche T*, et al.* Structural and Functional Characterization of the Bacterial Type III Secretion Export Apparatus. *PLoS pathogens* **12**, e1006071 (2016).